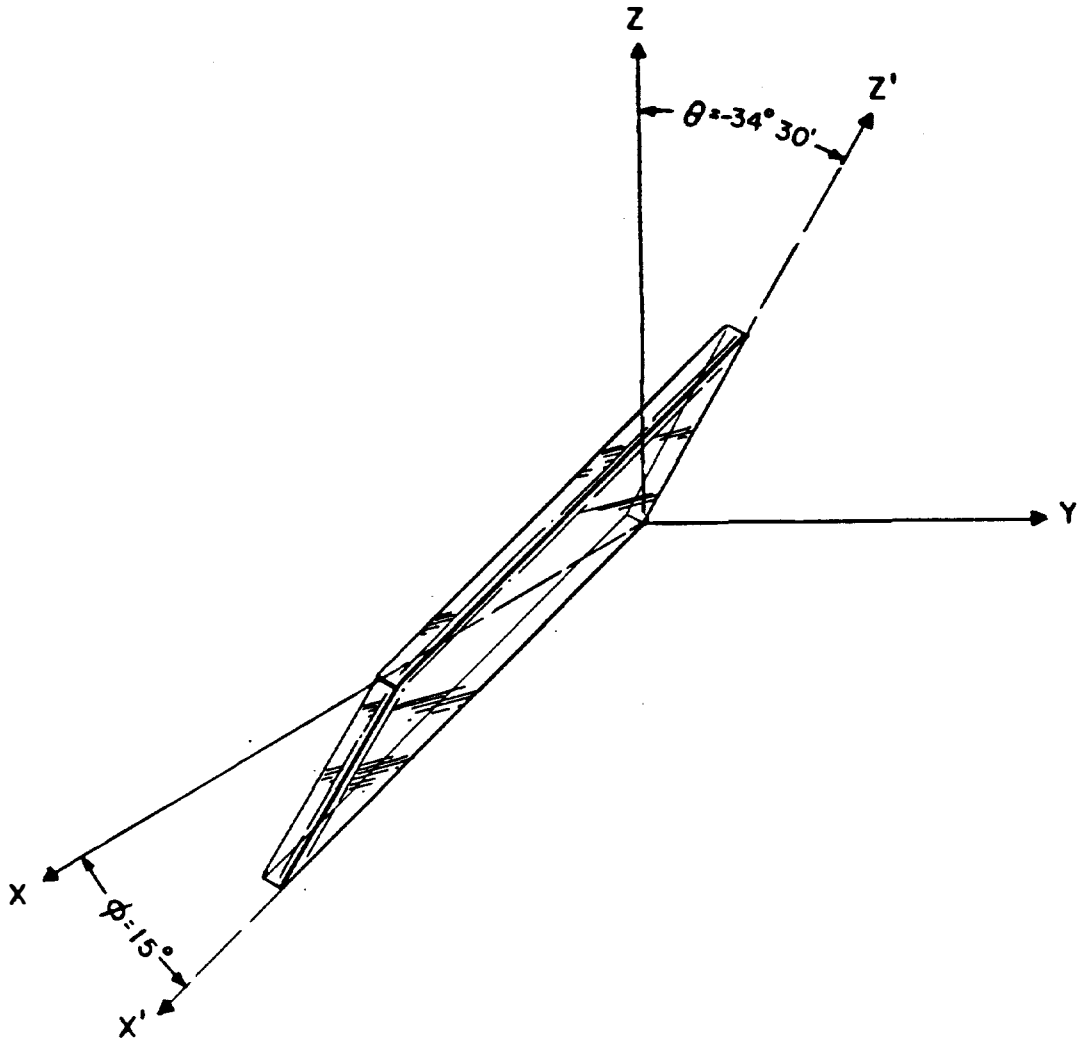

Fig. 2. Orientation of a quartz plate described by the angles ϕ and θ: Plate $\phi = 15°$, $\theta = -34°30'$.

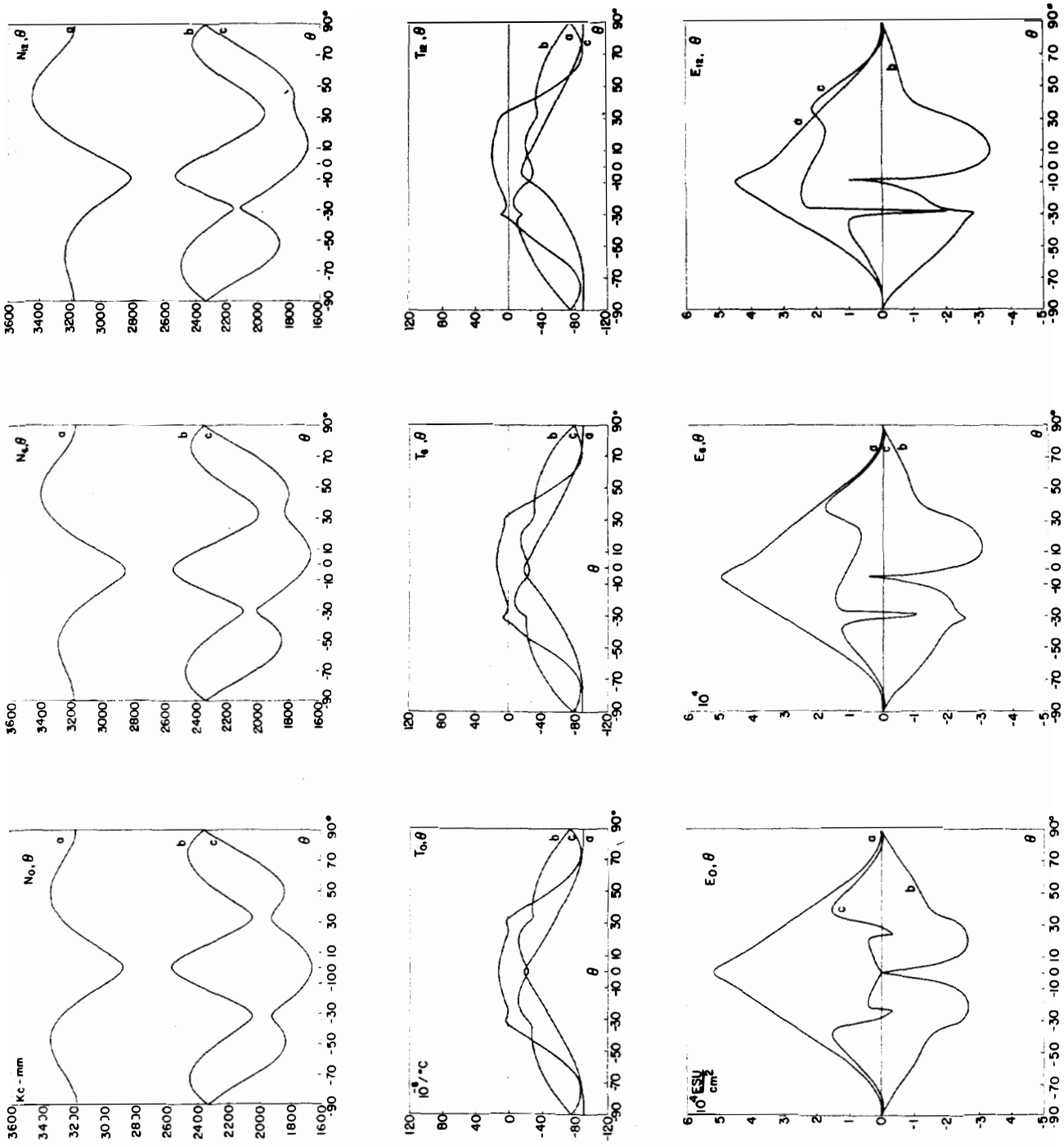

Fig. 3a Frequency constant N, piezoelectric constant e, and temperature coefficient of frequency (first order) Tf for quartz plates of different orientations vibrating in thickness modes.

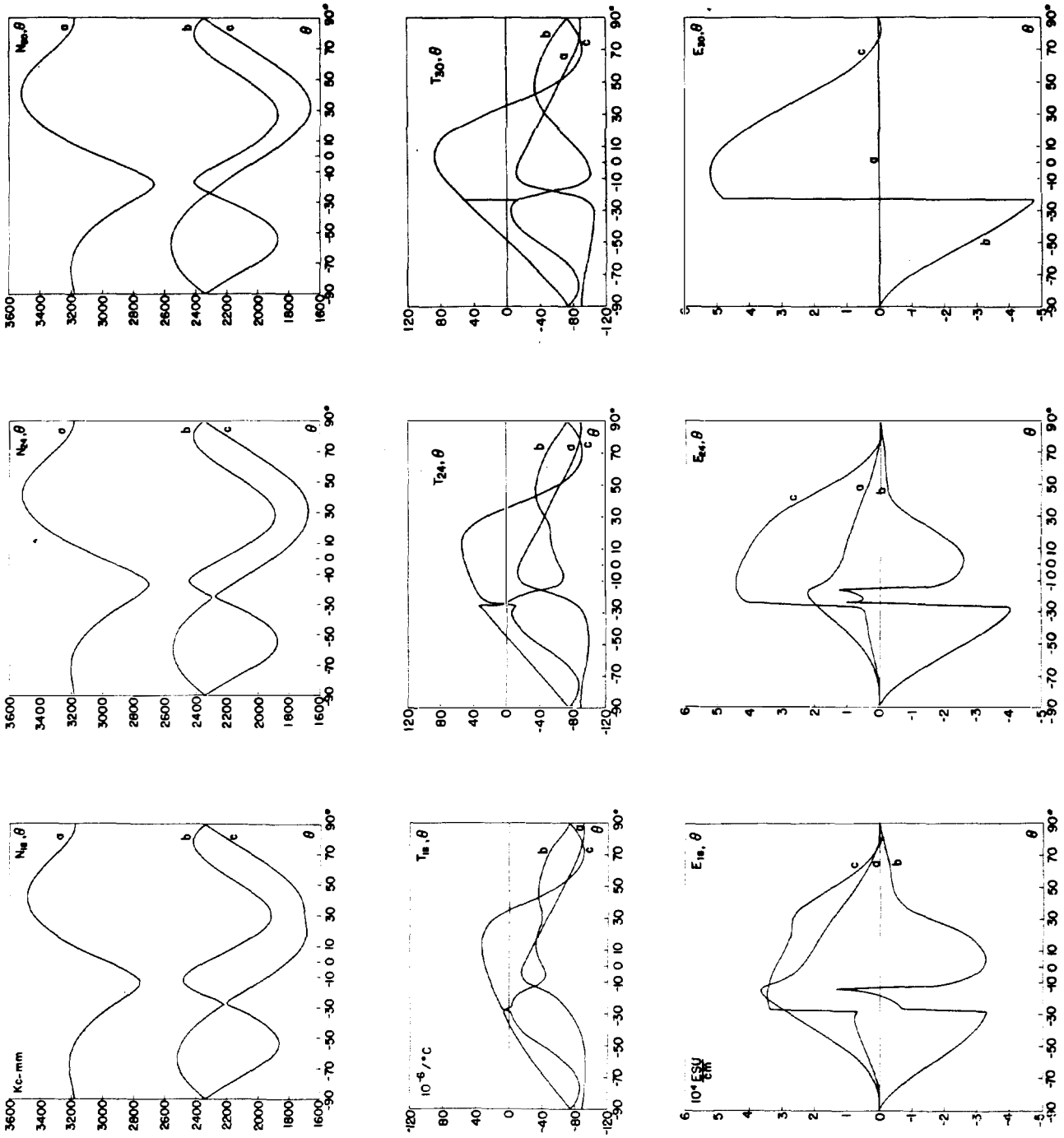

Fig. 3b Frequency constant N, piezoelectric constant e, and temperature coefficient of frequency (first order) Tf for quartz plates of different orientations vibrating in thickness modes.

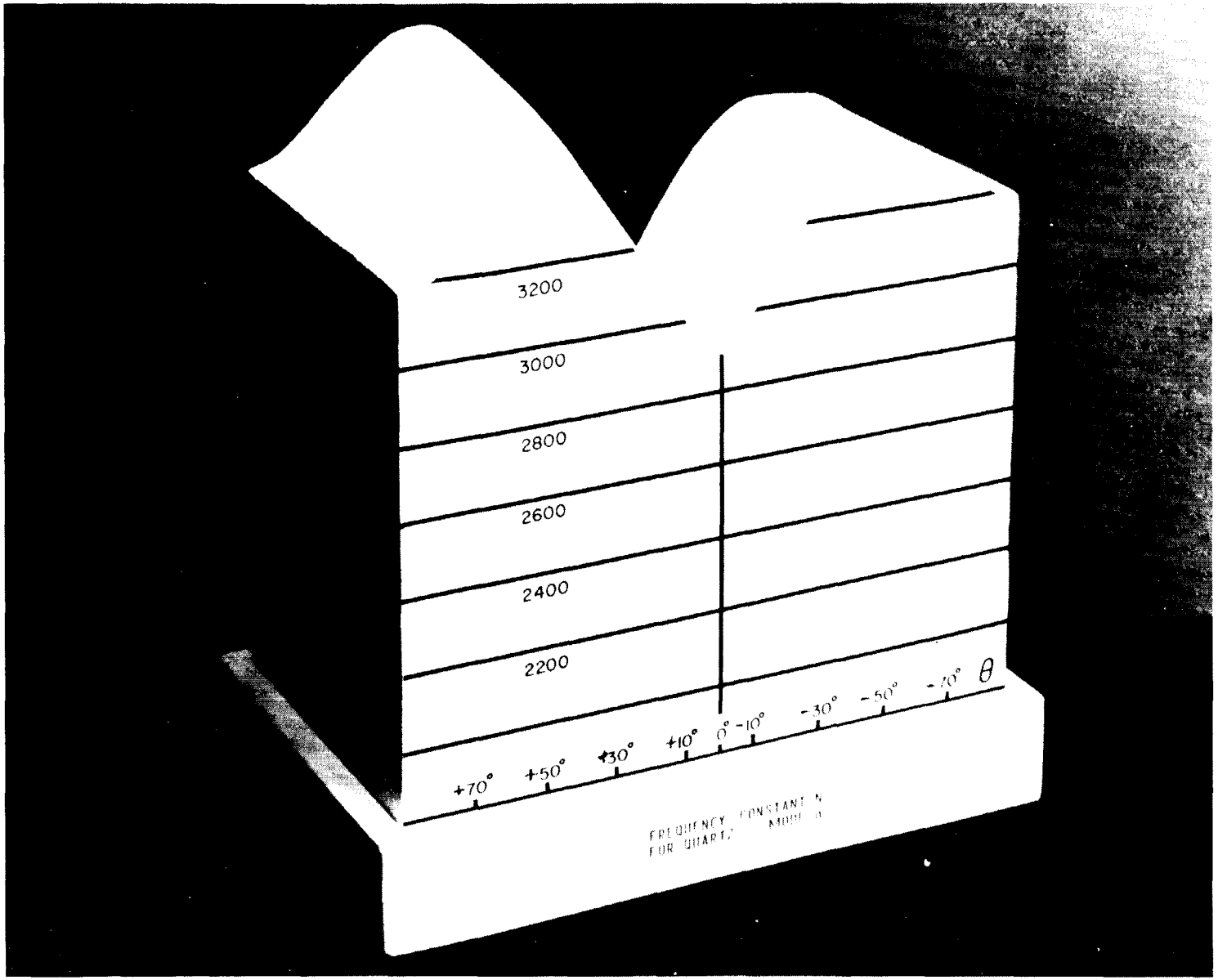

Fig. 4 Model of the frequency constant N for quartz plates of different orientations vibrating in the thickness mode A (Photograph)

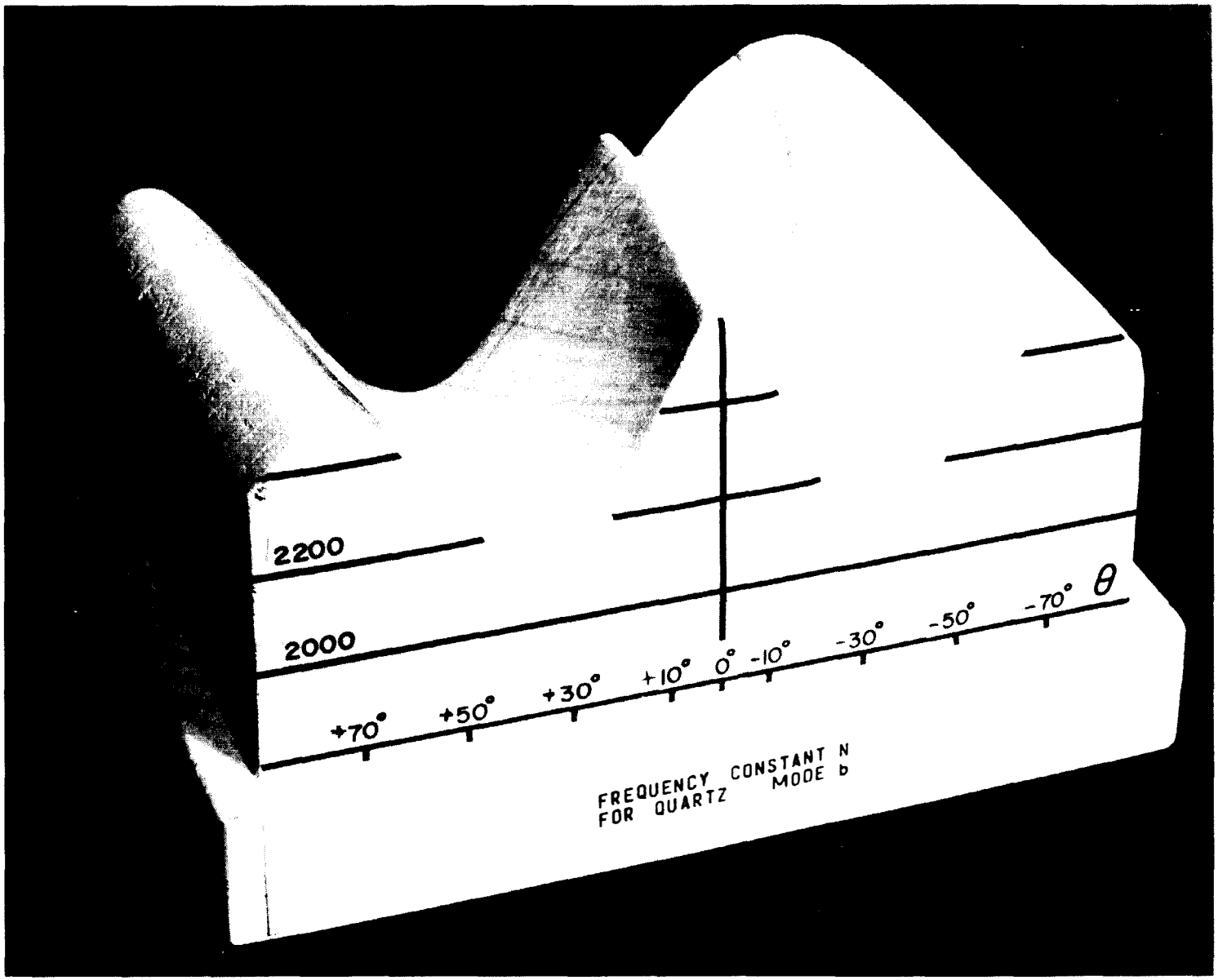

Fig. 5 Model of the frequency constant N for quartz plates of different orientations vibrating in the thickness mode B (Photograph)

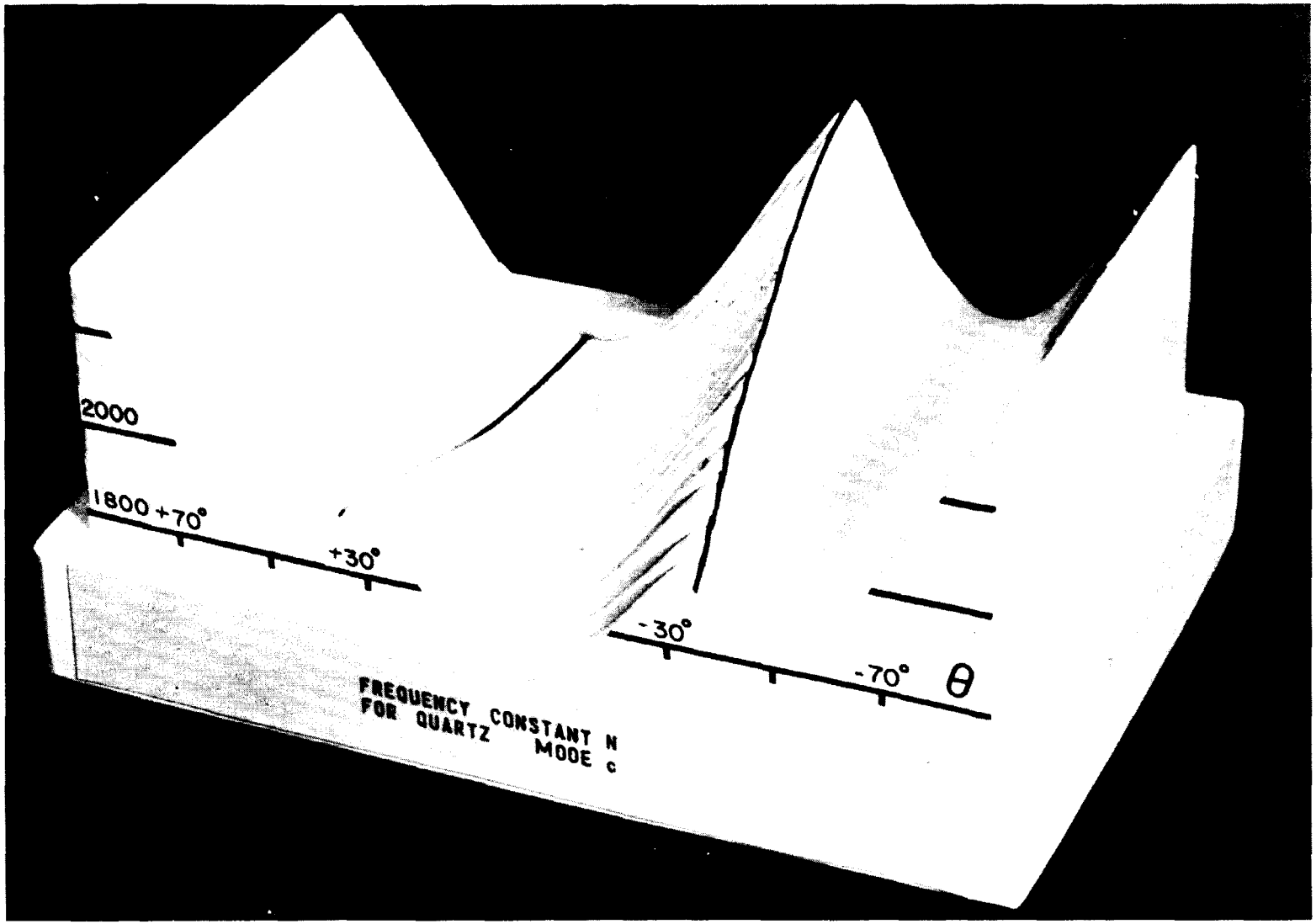

Fig. 6 Model of the frequency constant N for quartz plates of different orientations vibrating in the thickness mode C (Photograph)

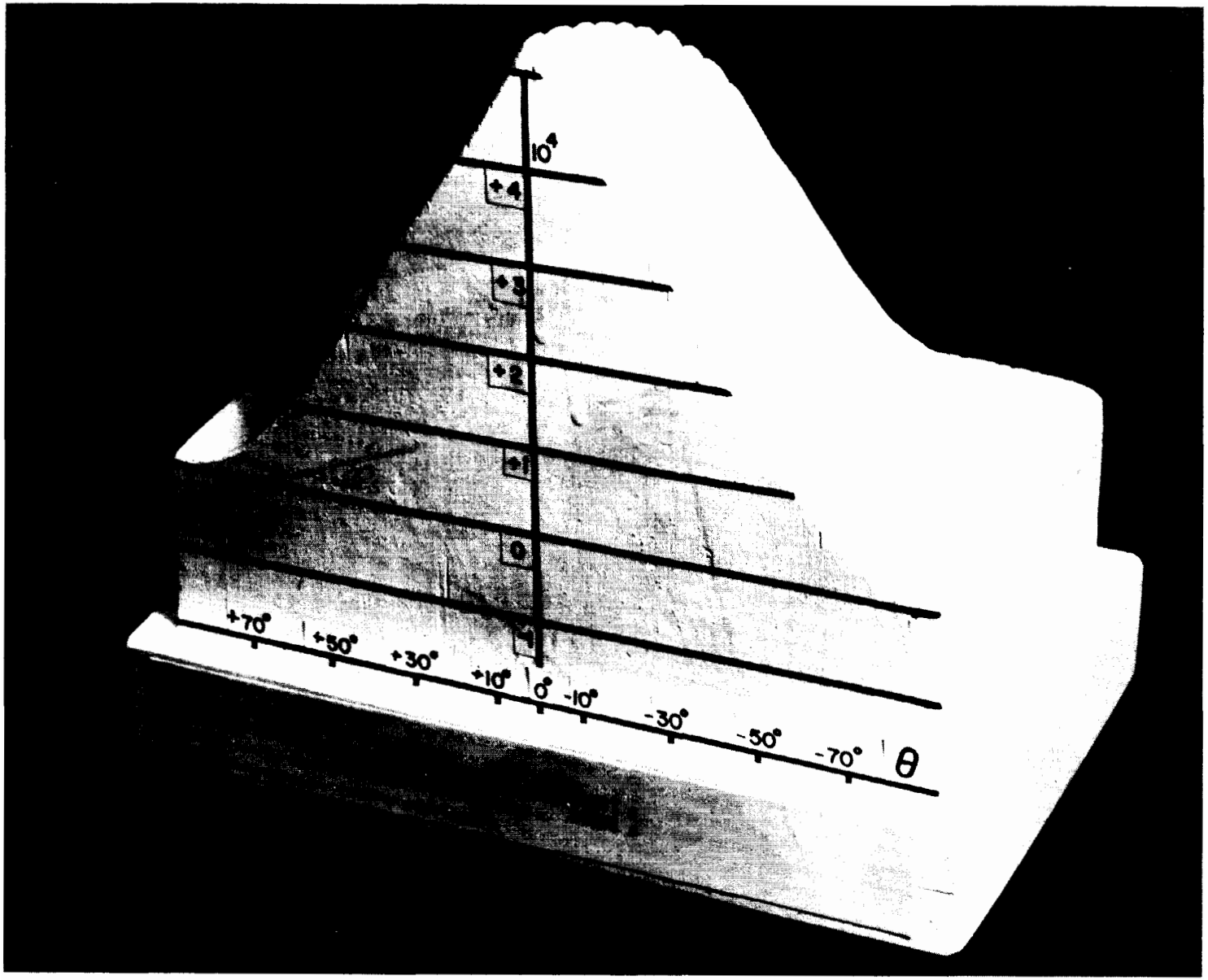

Fig. 7 Model of the piezoelectric constant e for quartz plates of different orientations viratin, in the thickness mode A (Photograph)

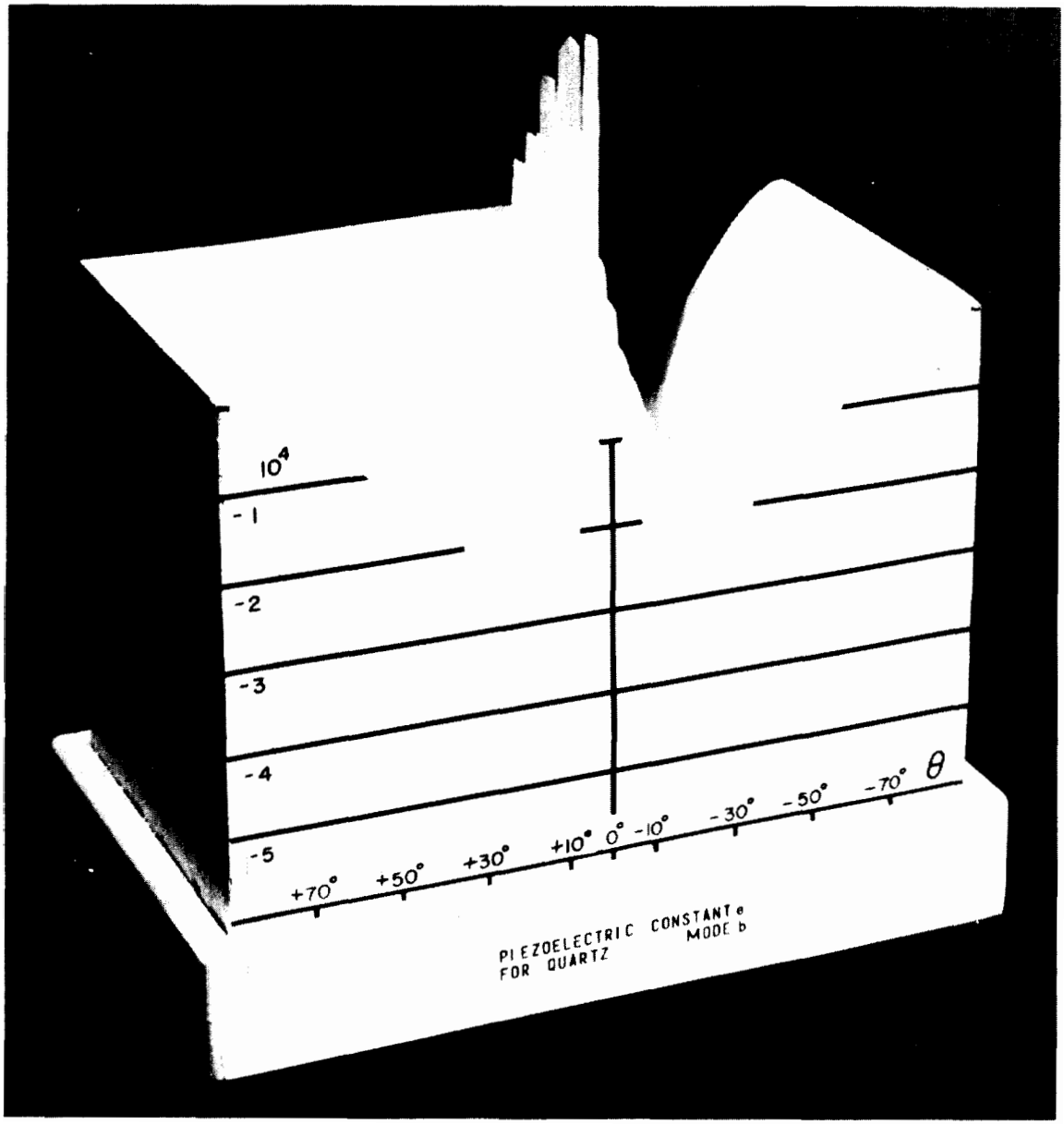

Fig. 8 Model of the piezoelectric constant e for quartz plates of different orientations vibrating in the thickness mode B (Photograph)

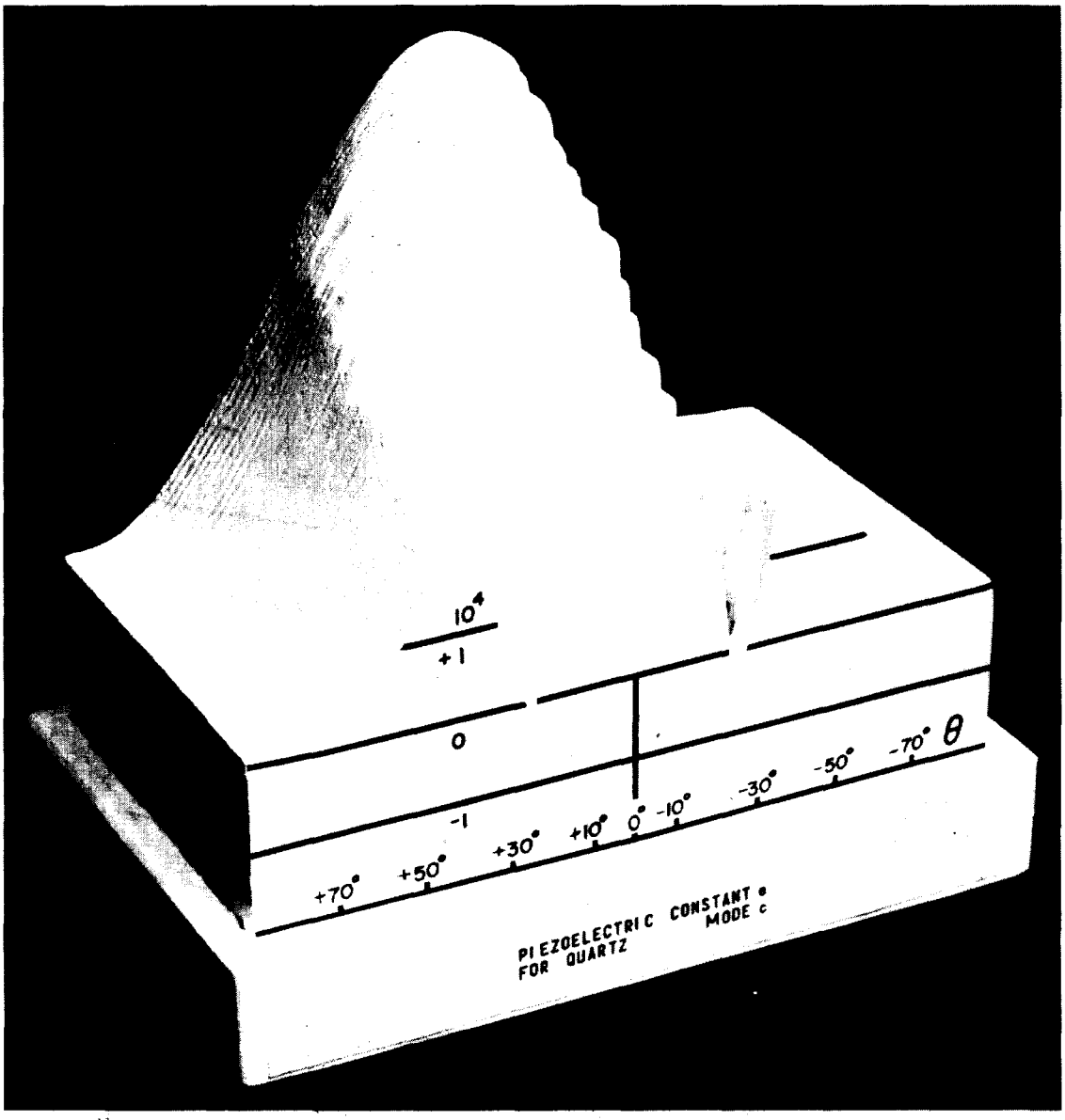

Fig. 9 Model of the piezoelectric constant e for quartz plates of different orientations vibrating in the thickness mode C (Photograph)

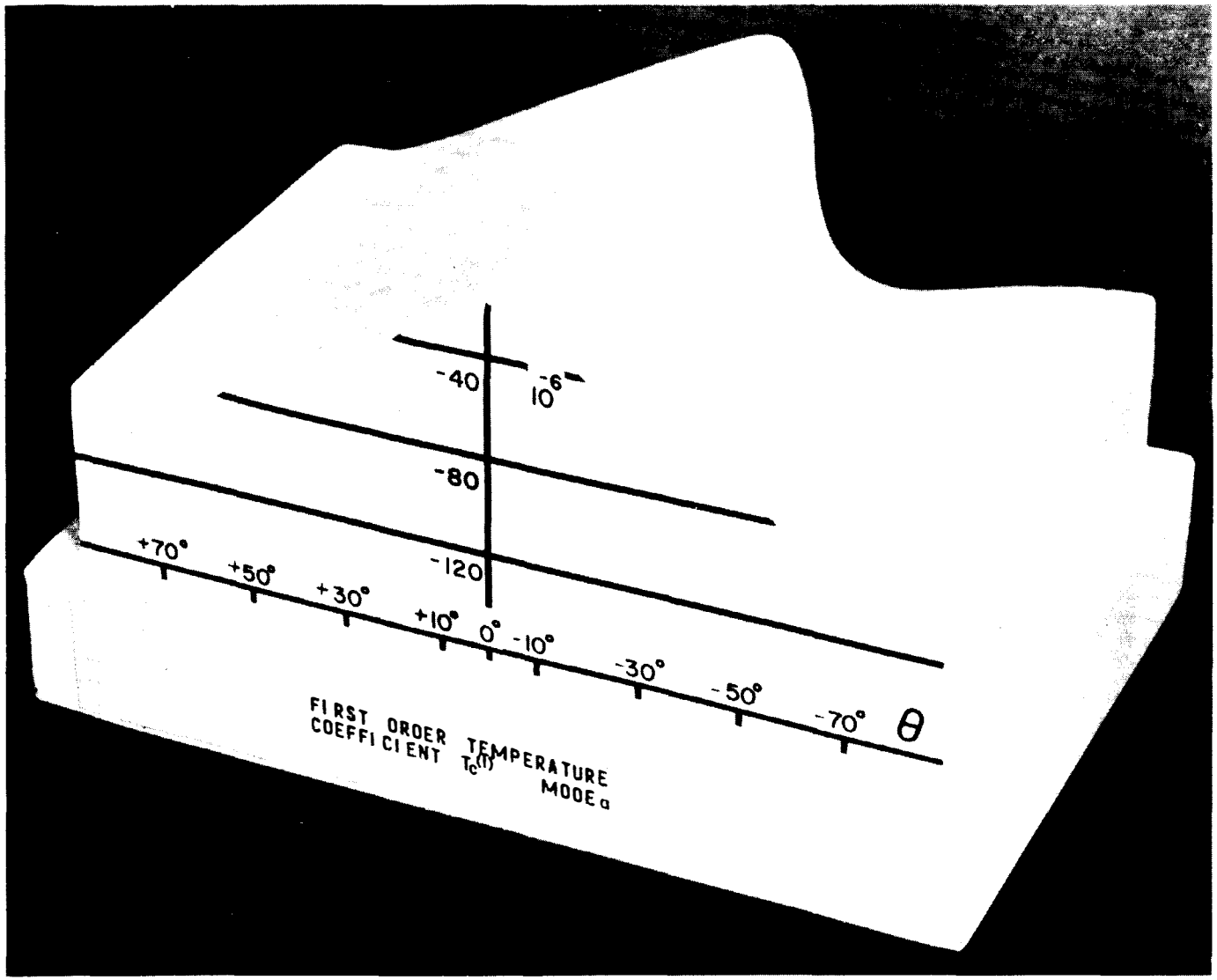

Fig. 10 Model of the temperature coefficient of frequency first order $T_c^{(1)}$ for quartz plates of different orientations vibrating in the thickness mode A (Photograph)

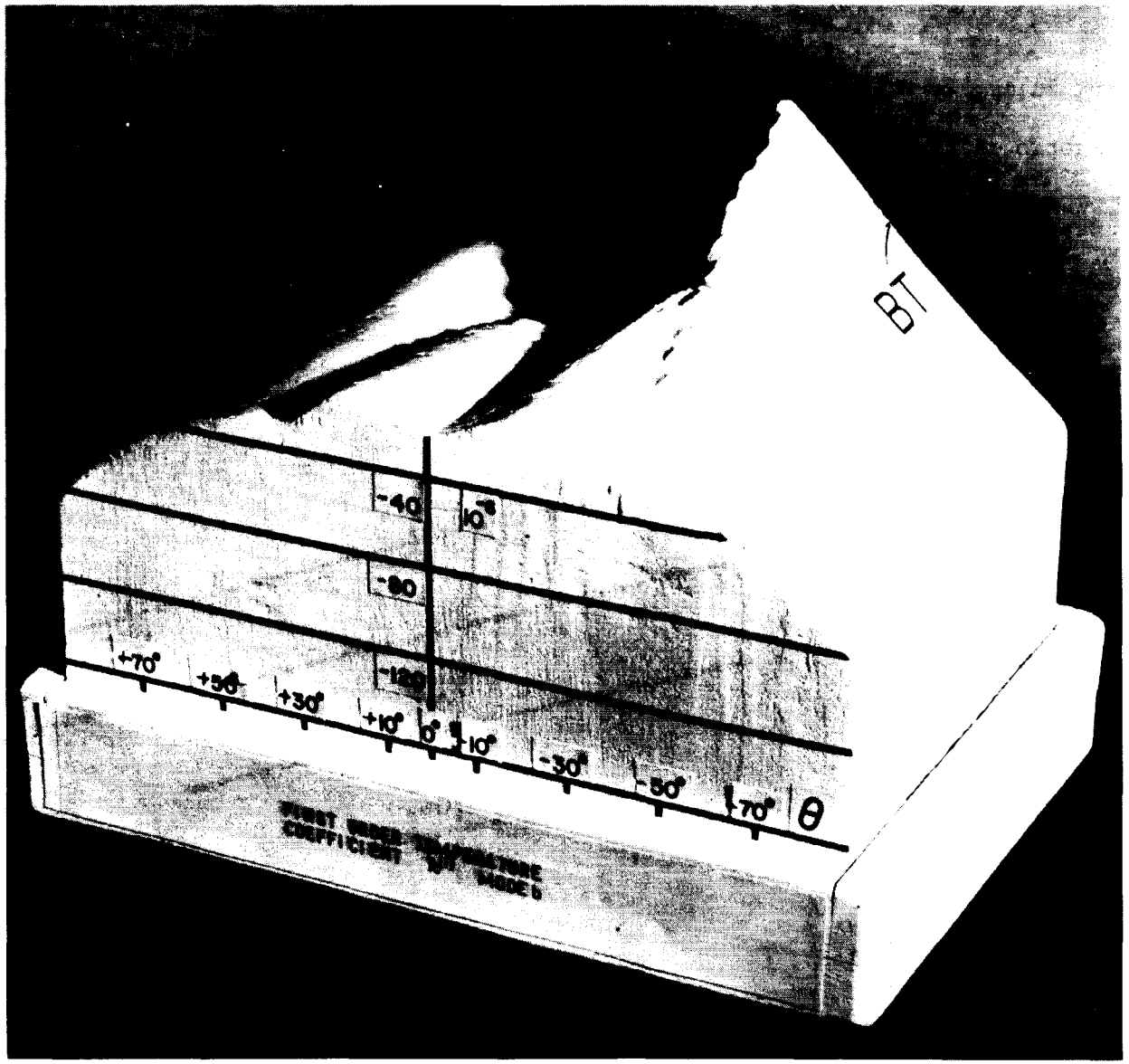

Fig. 11 Model of the temperature coefficient of frequency first order $T_c^{(1)}$ for quartz plates of different orientations vibrating in the thickness mode B (Photograph)

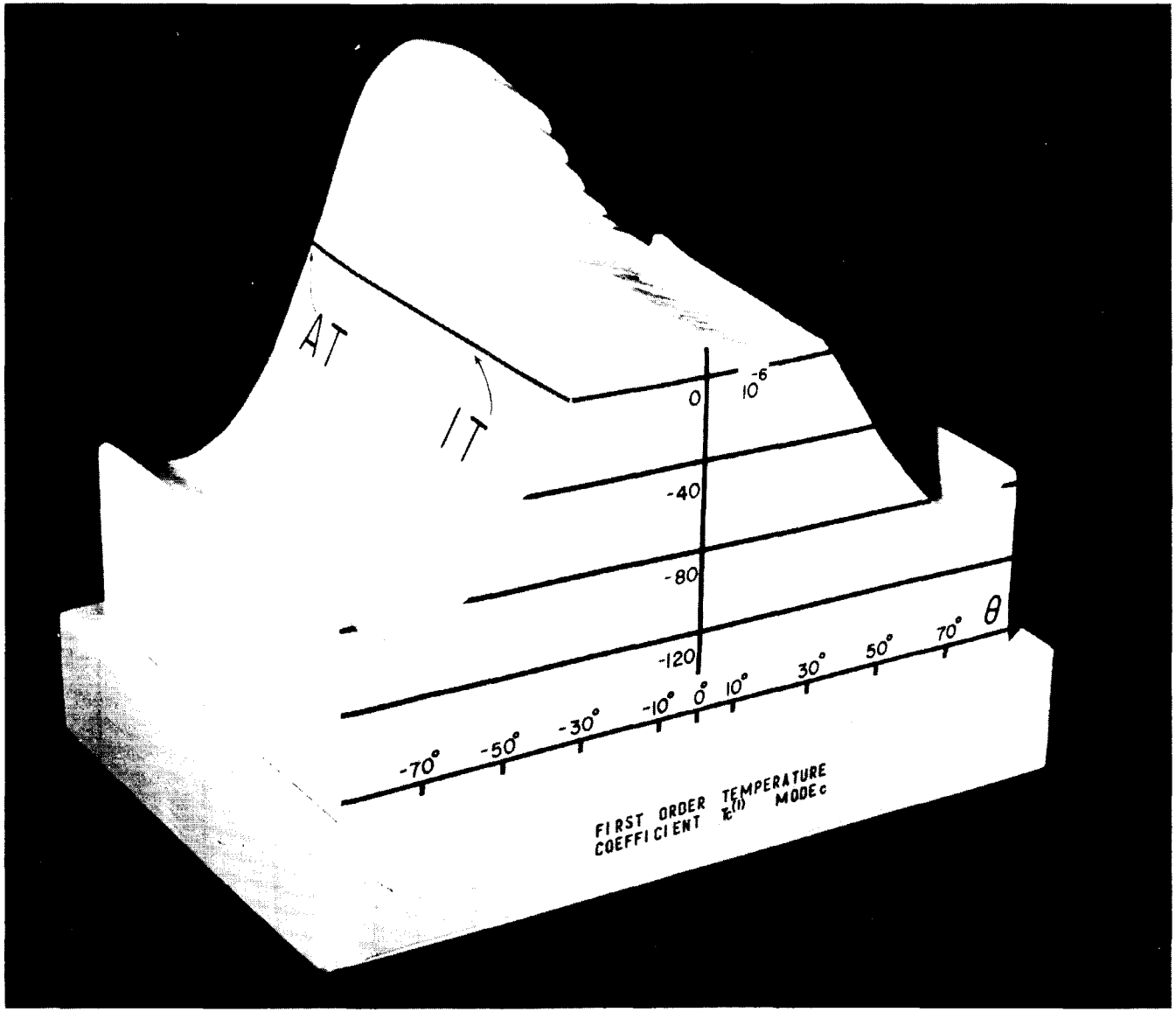

Fig. 12 Model of the temperature coefficient of frequency first order $T_c^{(1)}$ for quartz plates of different orientations vibrating in the thickness mode C (Photograph)

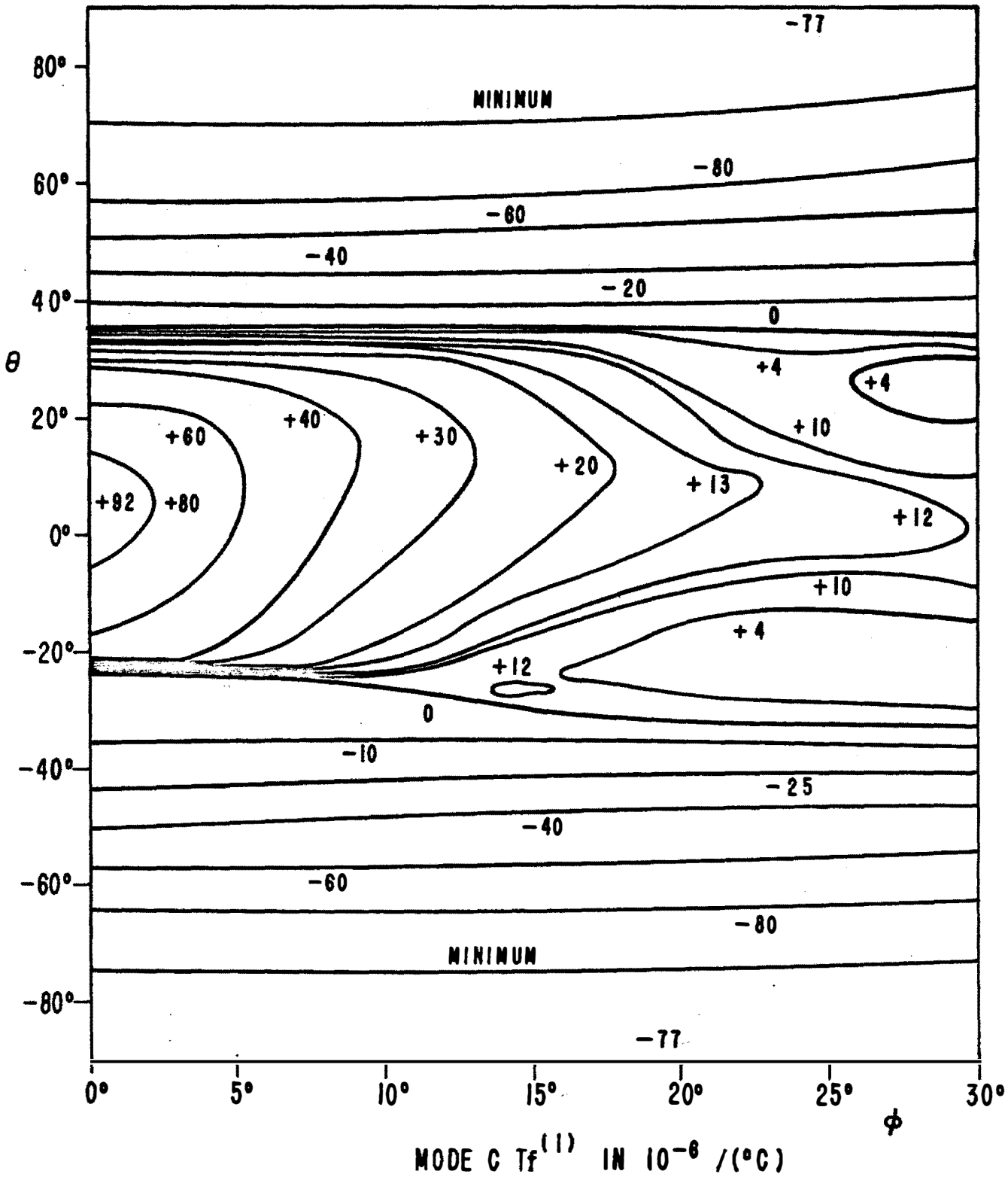

Fig. 13 First-order temperature coefficient of frequency for the C mode: Altitude Chart

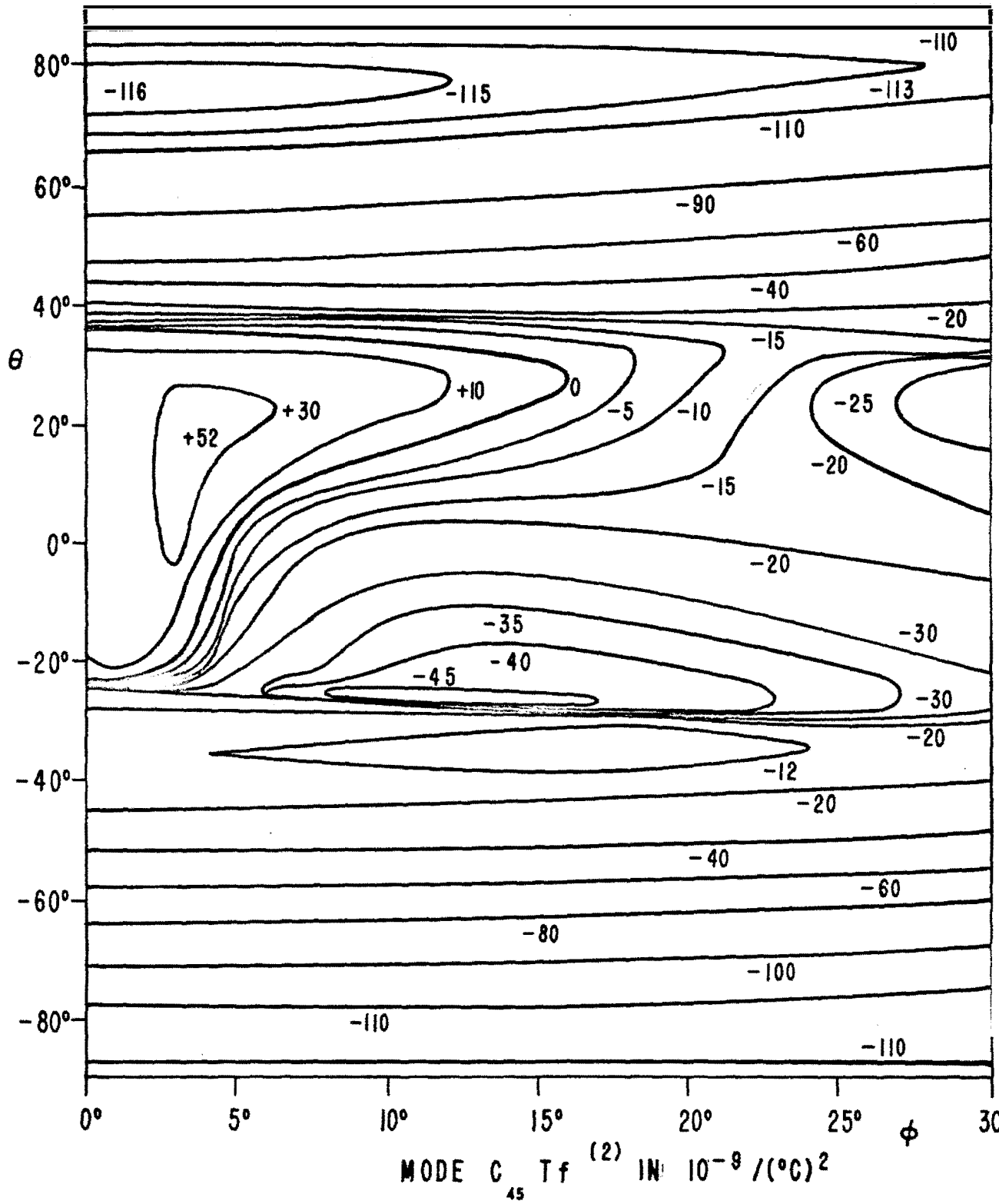

Fig. 14 Second-order temperature coefficient of frequency for the C mode: Altitude Chart

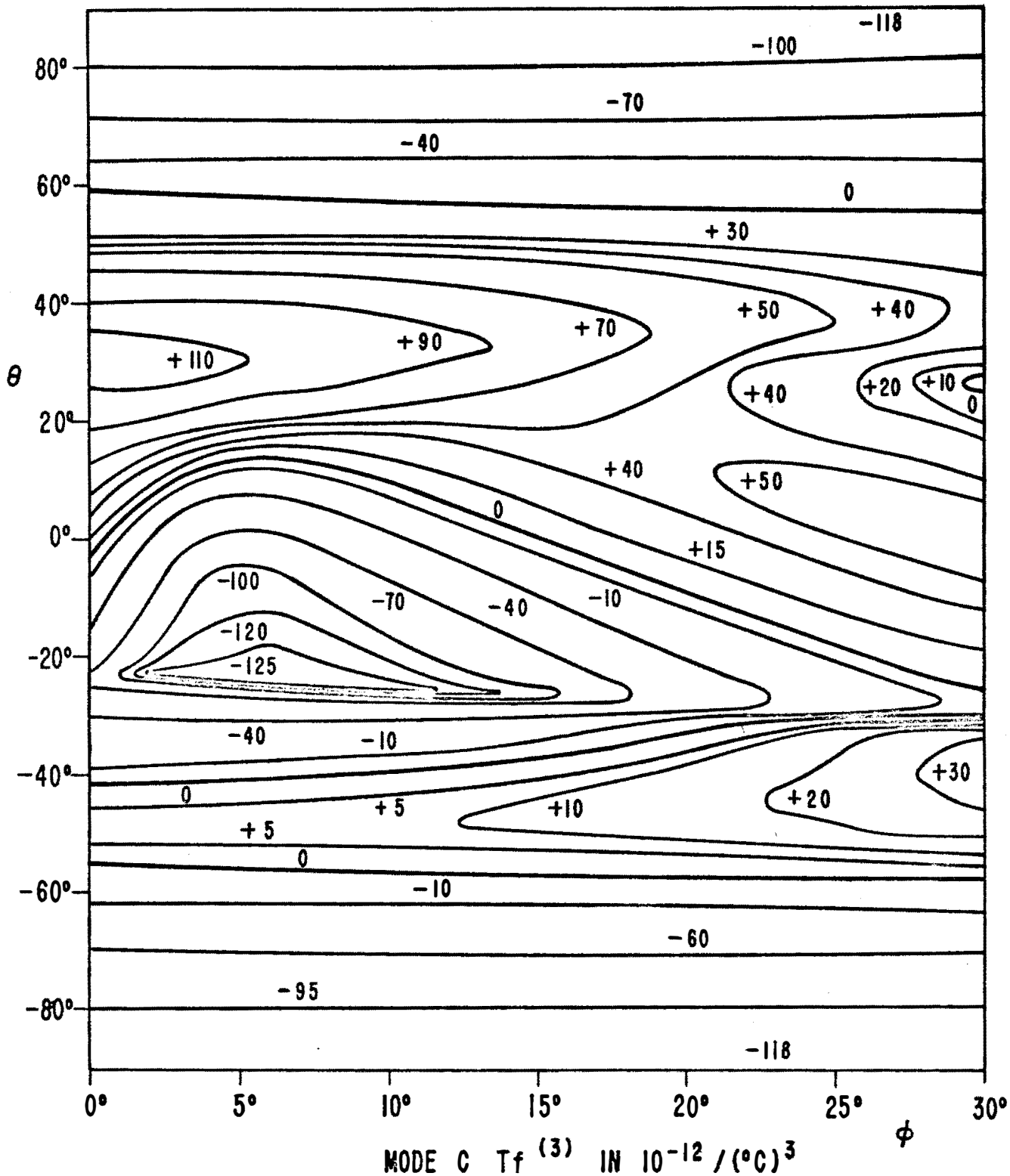

Fig. 15 Third-order temperature coefficient of frequency for the C mode: Altitude Chart

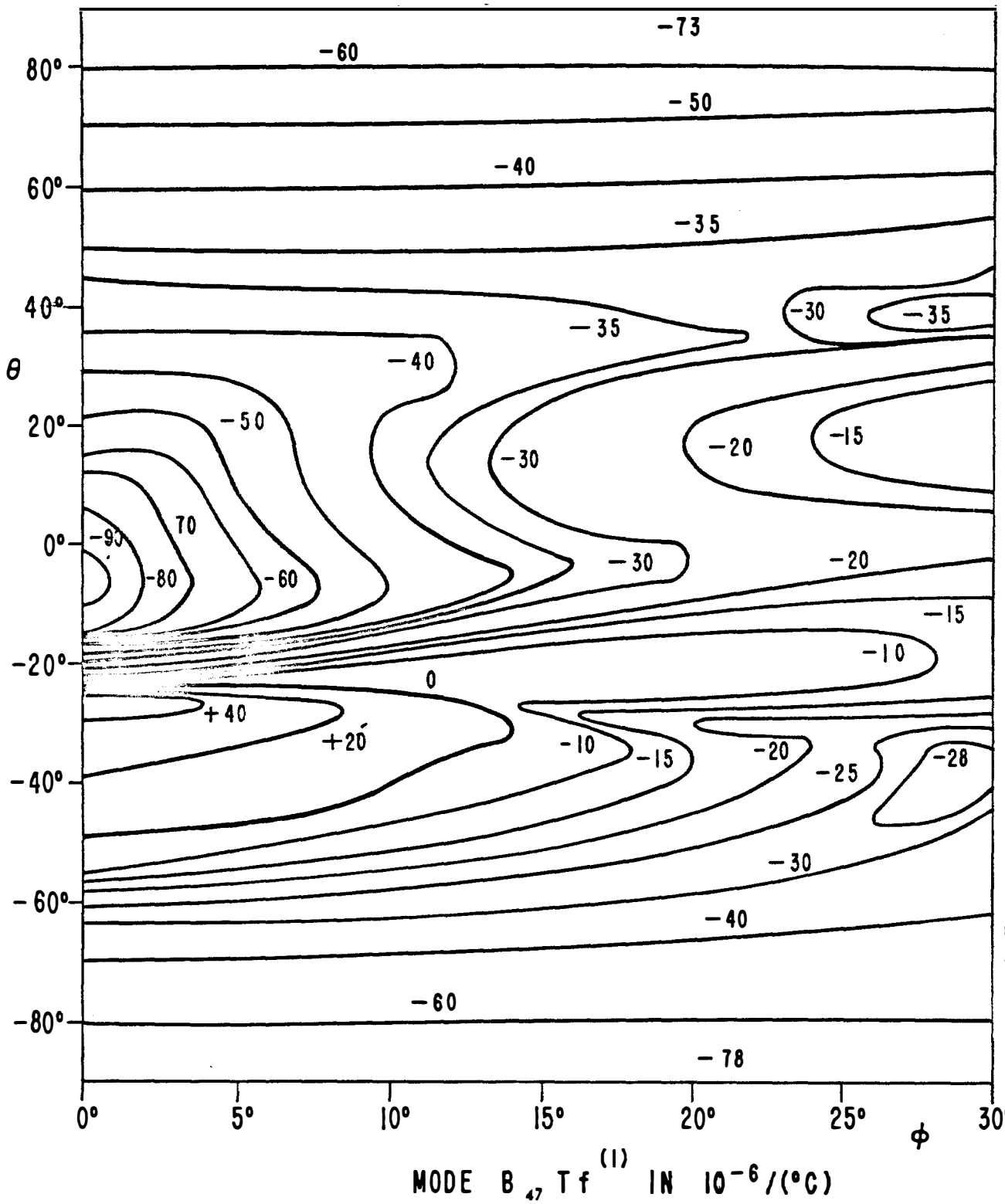

Fig. 16 First-order temperature coefficient of frequency for the B mode: Altitude Chart

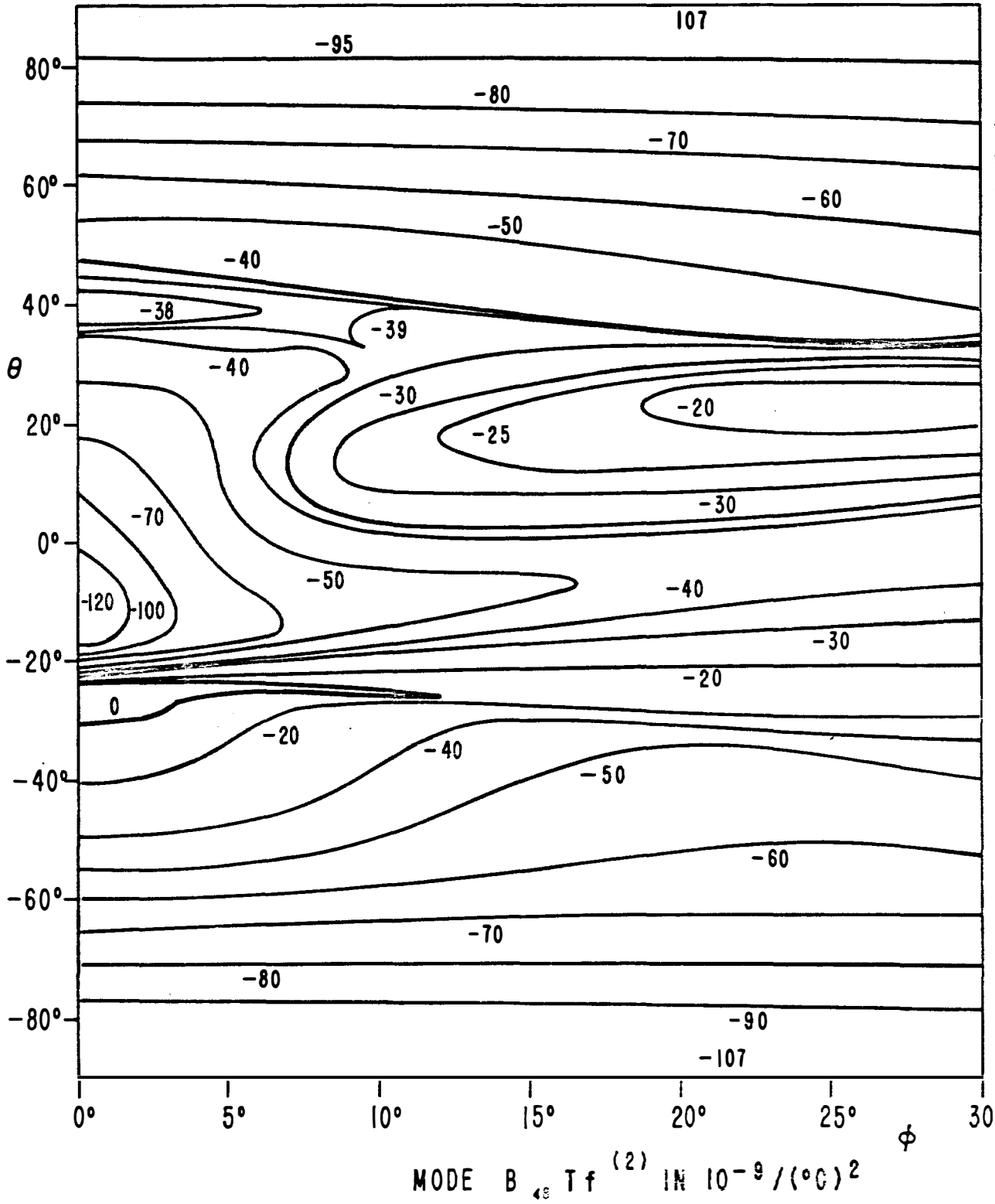

Fig. 17 Second-order temperature coefficient of frequency for the B mode: Altitude Chart

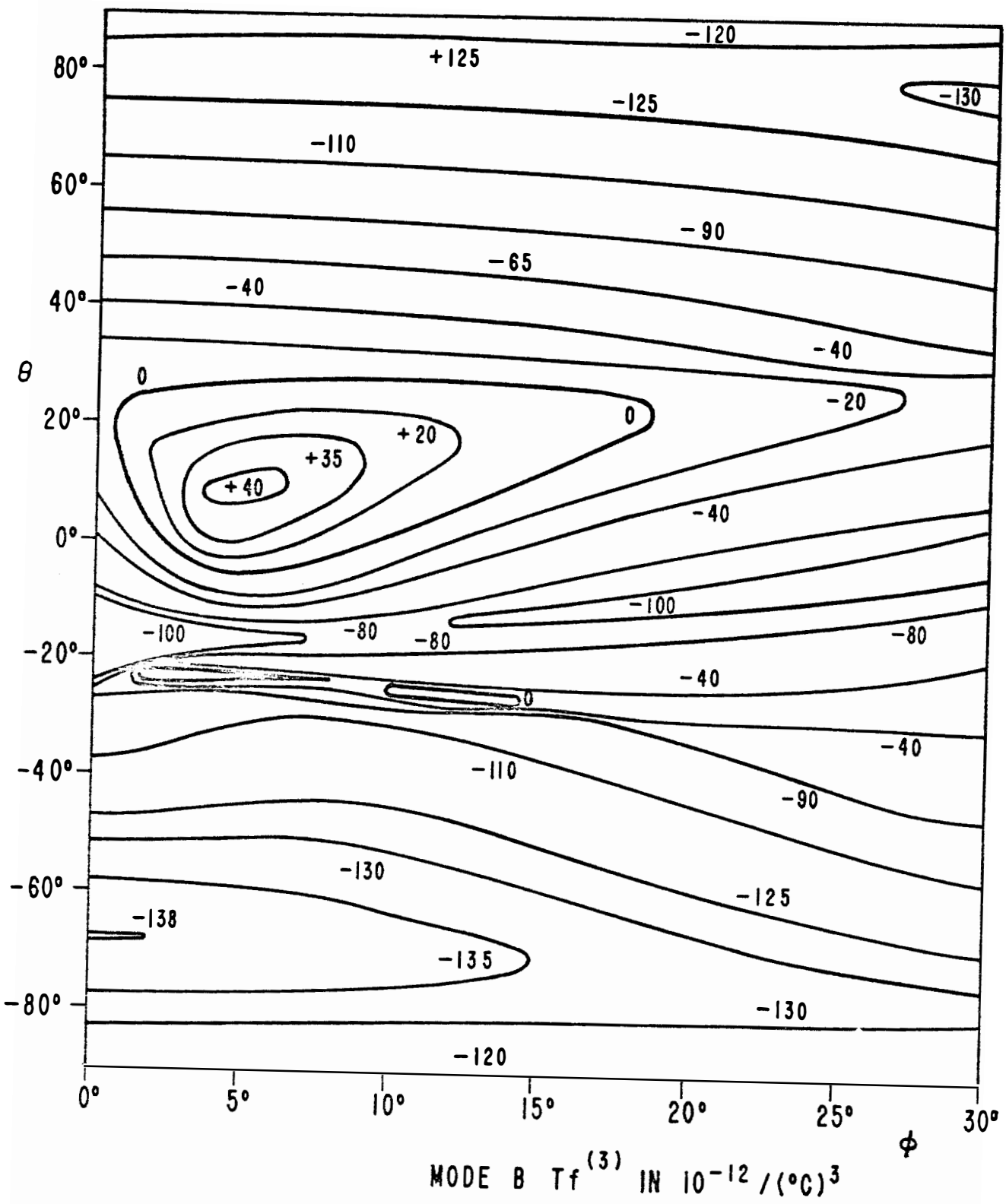

Fig. 19 Third-order temperature coefficient of frequency for the B mode: Altitude Chart

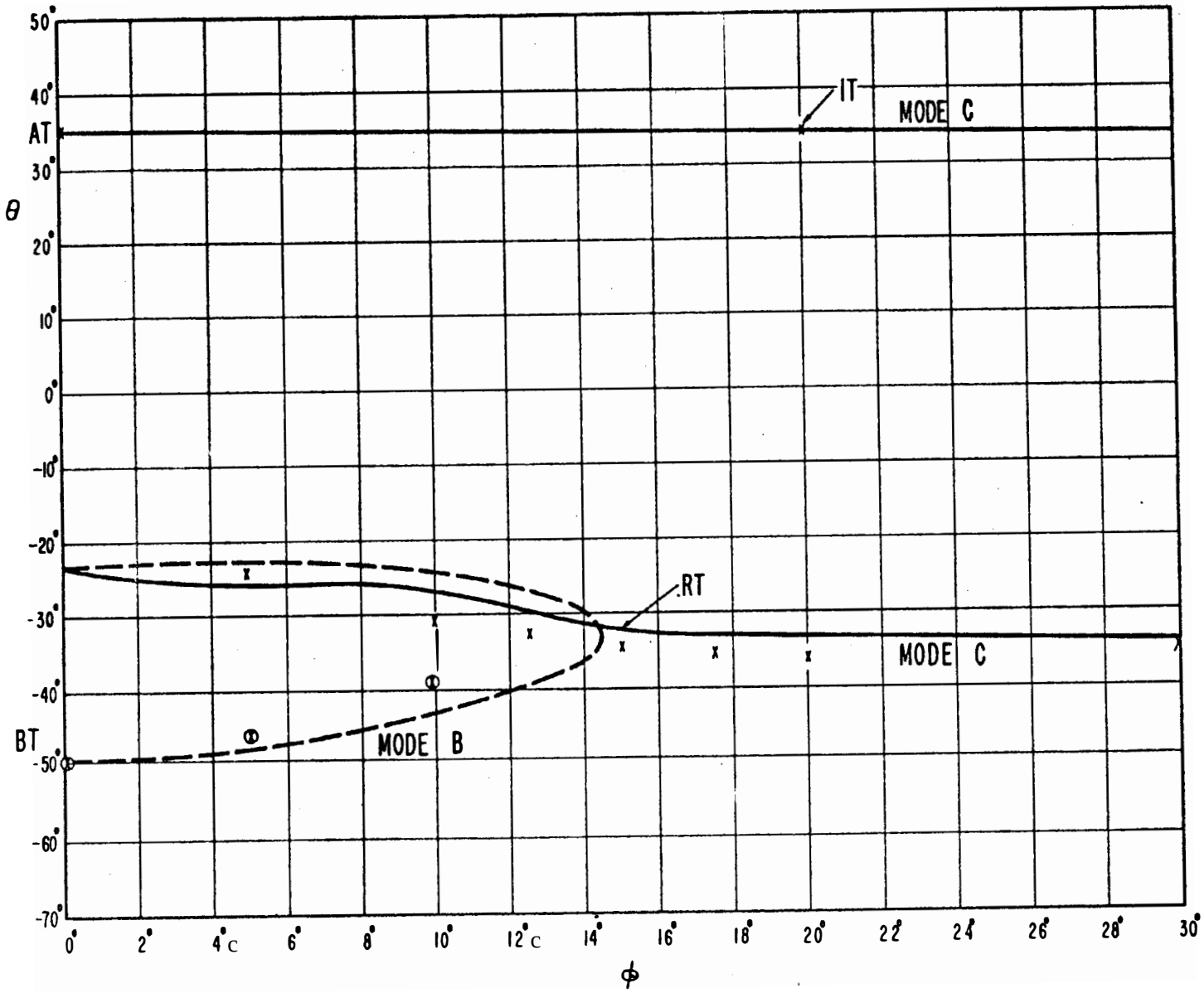

Fig. 19. Locus of $Tf^{(1)} = 0$ for the thickness modes B and C of quartz plates as a function of the angles θ and ϕ in a rectangular coordinate system.

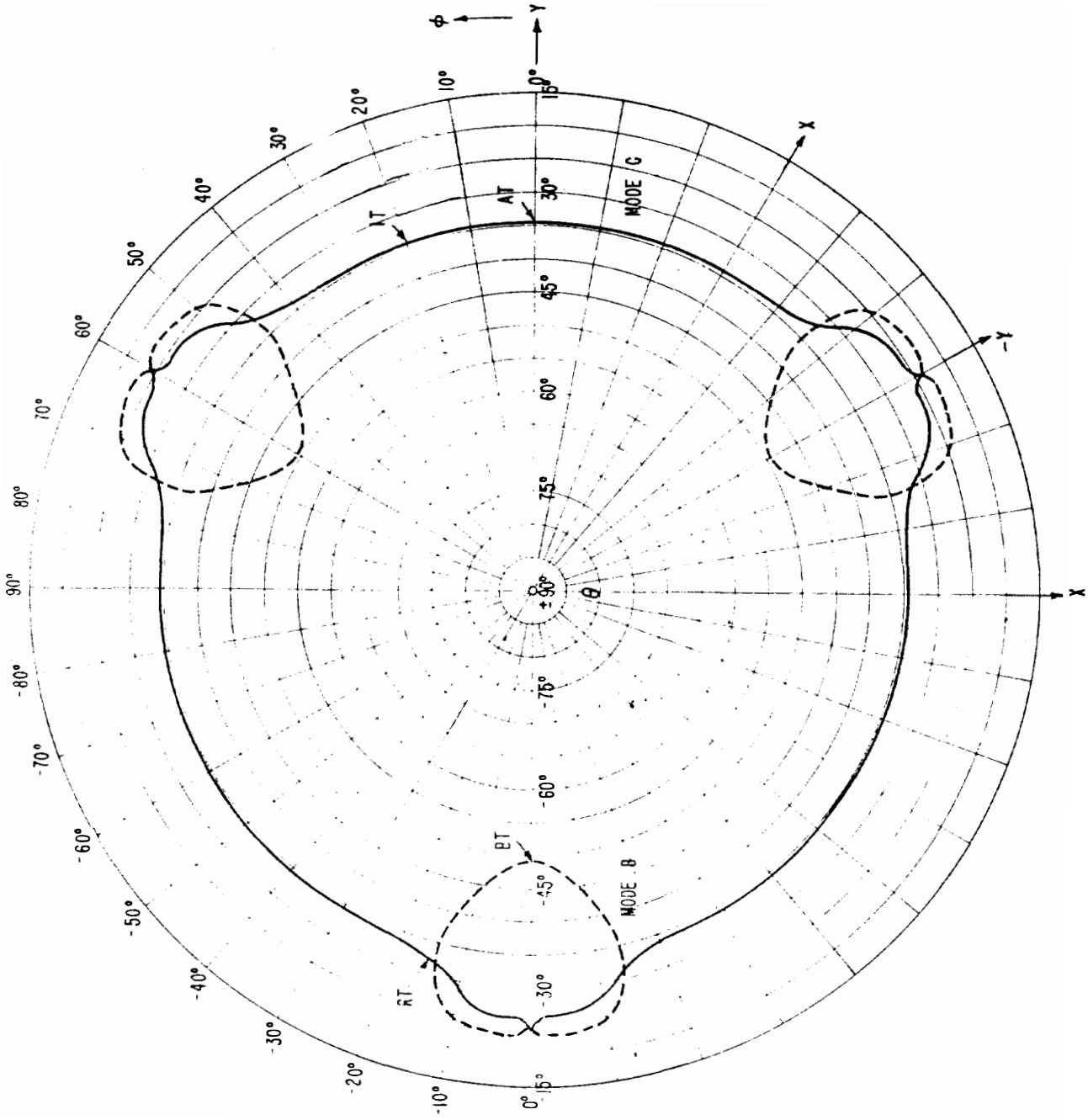

Fig. 20. Locus of $Tf^{(1)} = 0$ for the thickness modes B and C of quartz plates as a function of the angles θ and ϕ in a polar coordinate system.

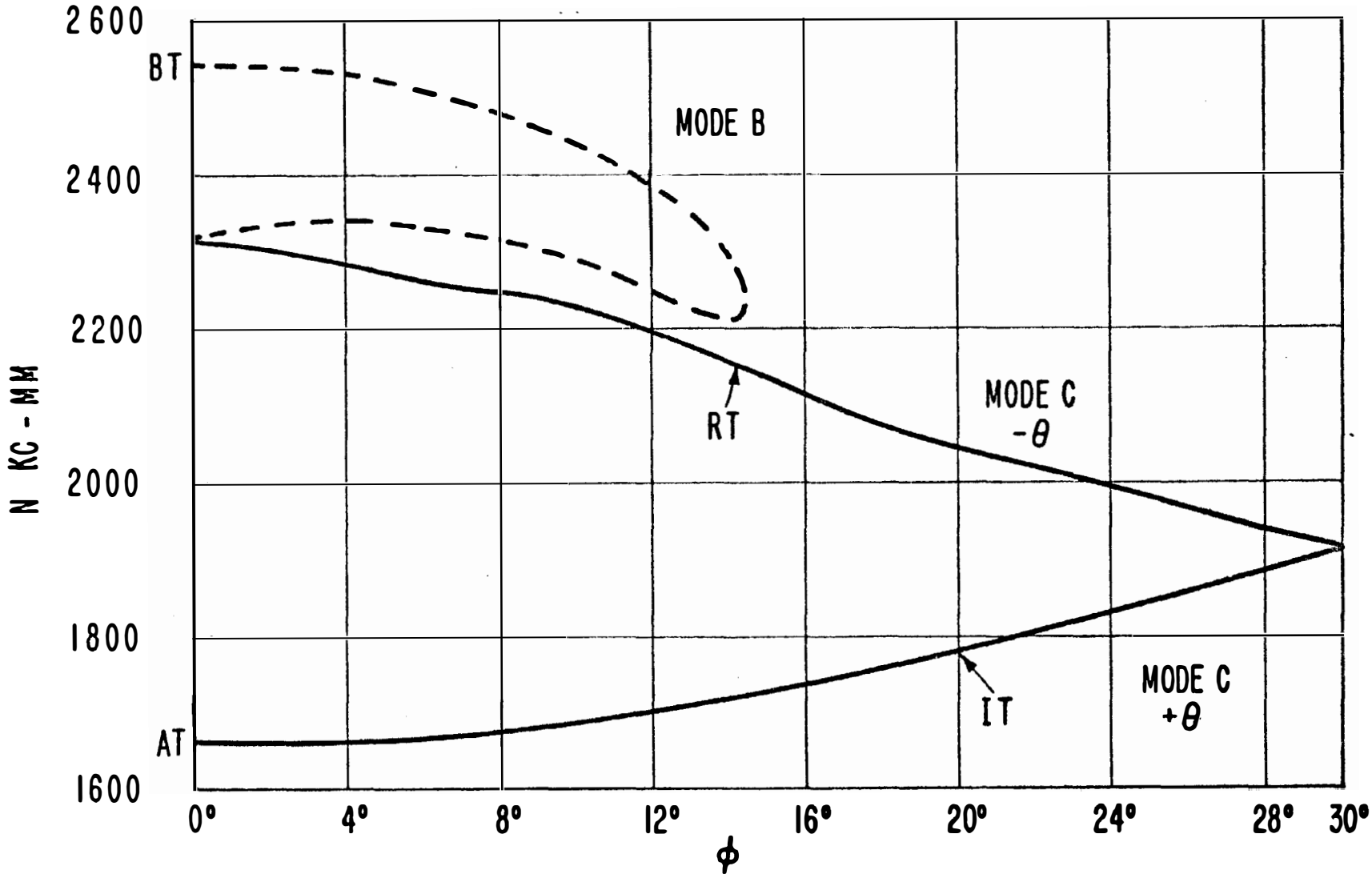

Fig. 21 Frequency constants of modes B and C when $Tf^{(1)} = 0$.

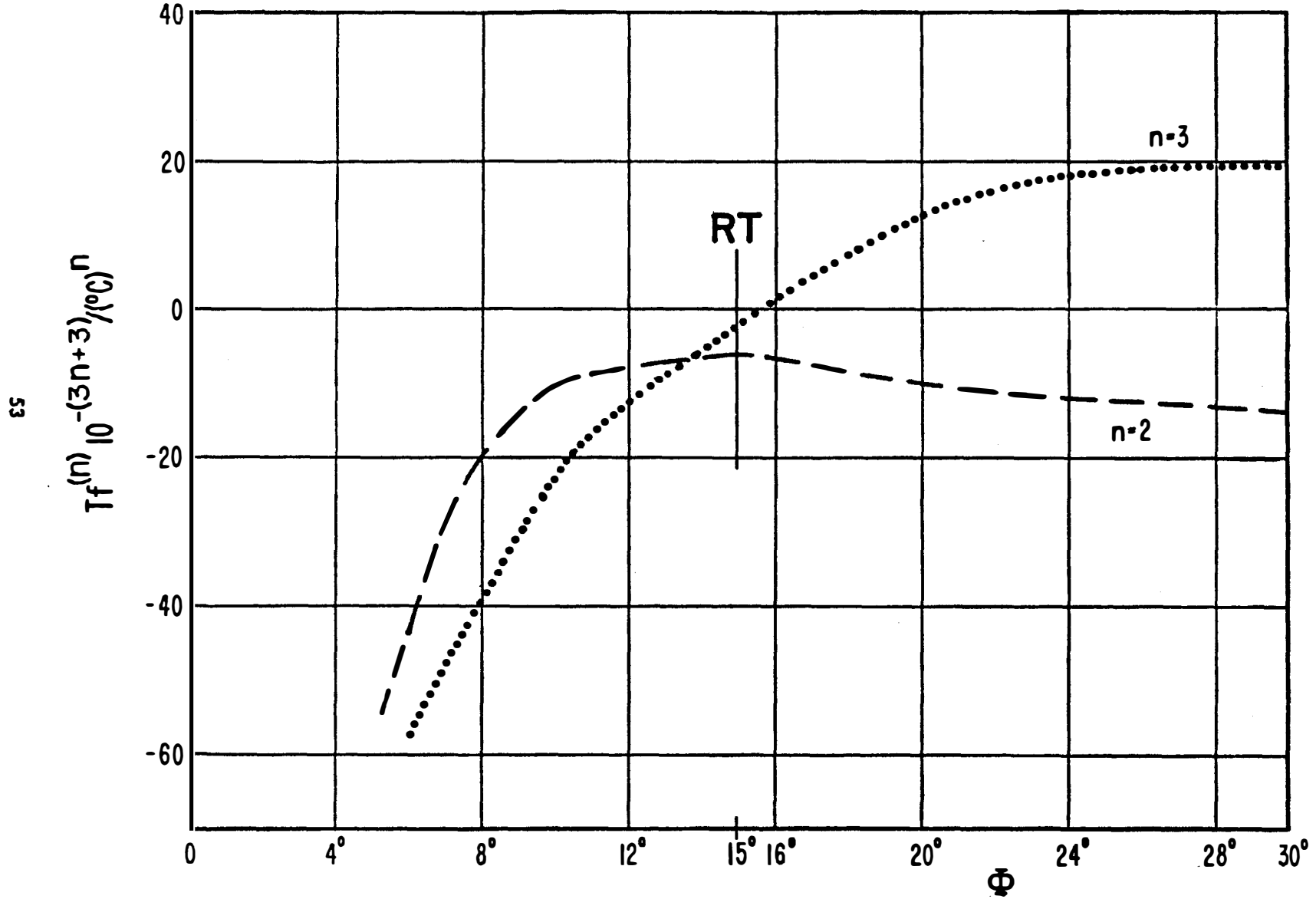

Fig. 22. Second-and third-order temperature coefficients of frequency for the thickness mode C when $Tf^{(1)} = 0$ for negative angles of θ.

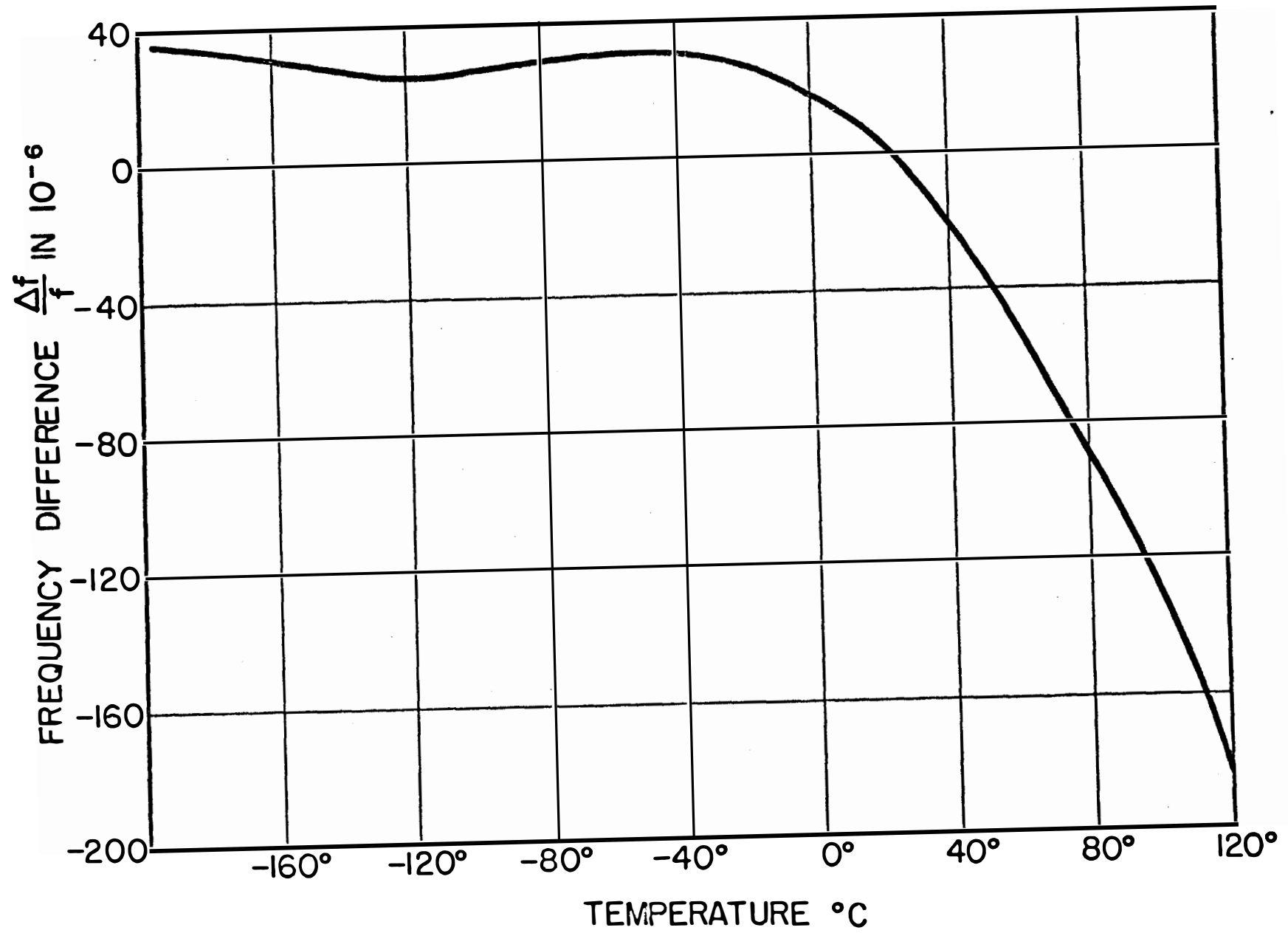

Fig. 23. Quartz cut (yxw ℓ) 10°, −32° having a small temperature dependence in the temperature range −200°C to 0°C.

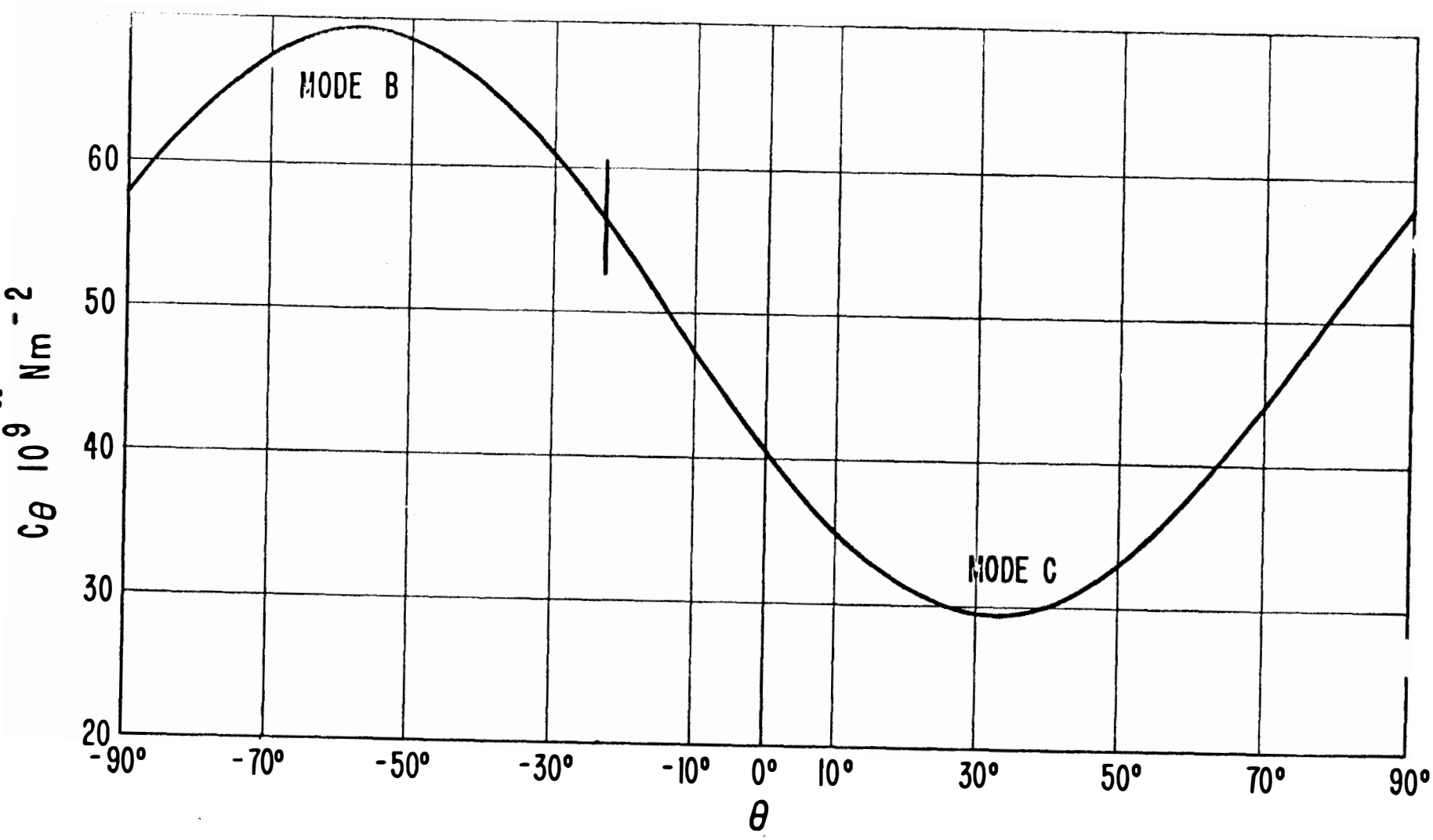

Fig. 24. Elastic stiffnesses c'_{55} (c'_{44}) for rotation (yxℓ) θ as a function of the angle θ.

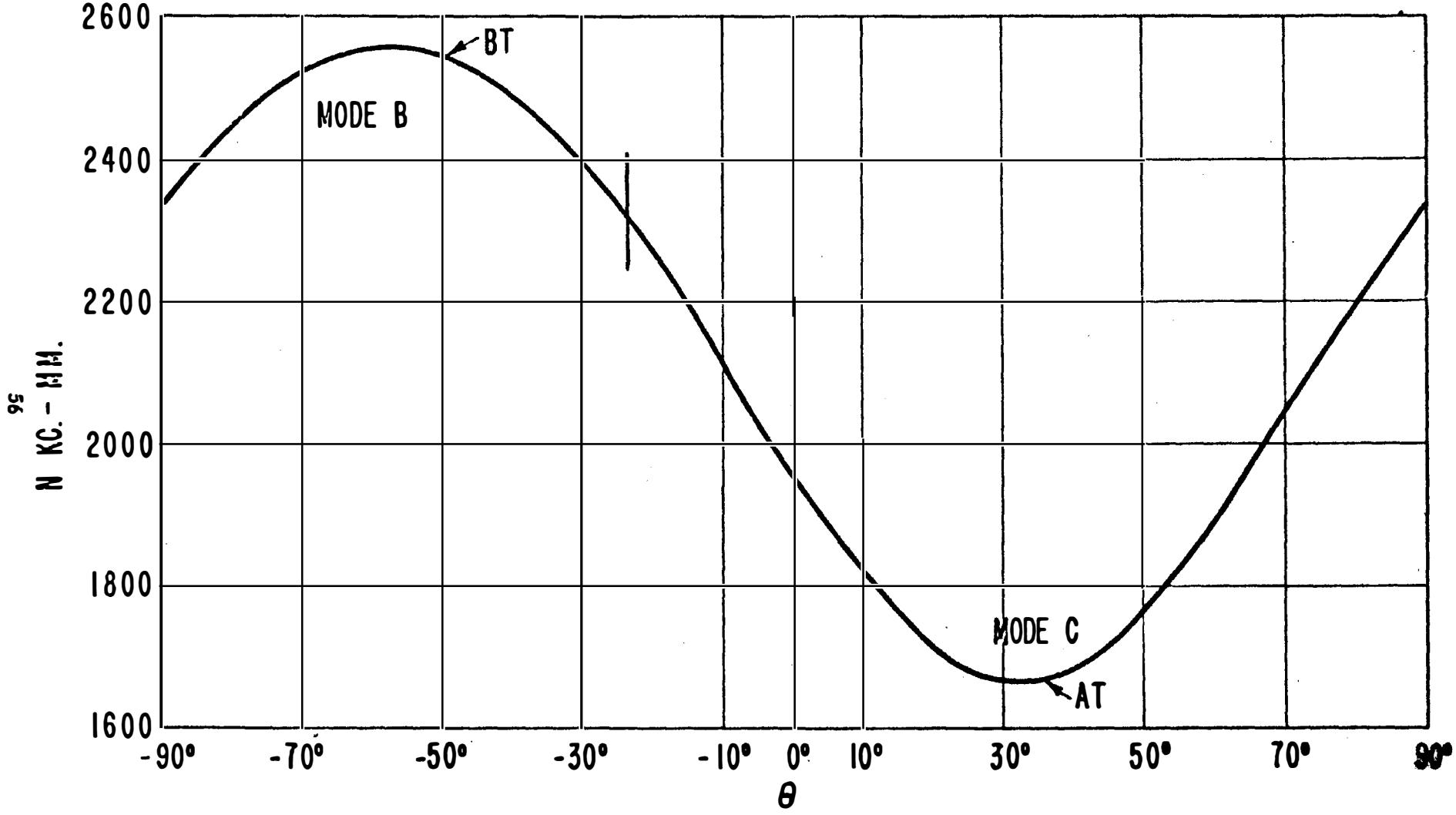

Fig. 25. Frequency constant N of the thickness-shear mode of the plate (yx ℓ) θ as a function of the angle θ.

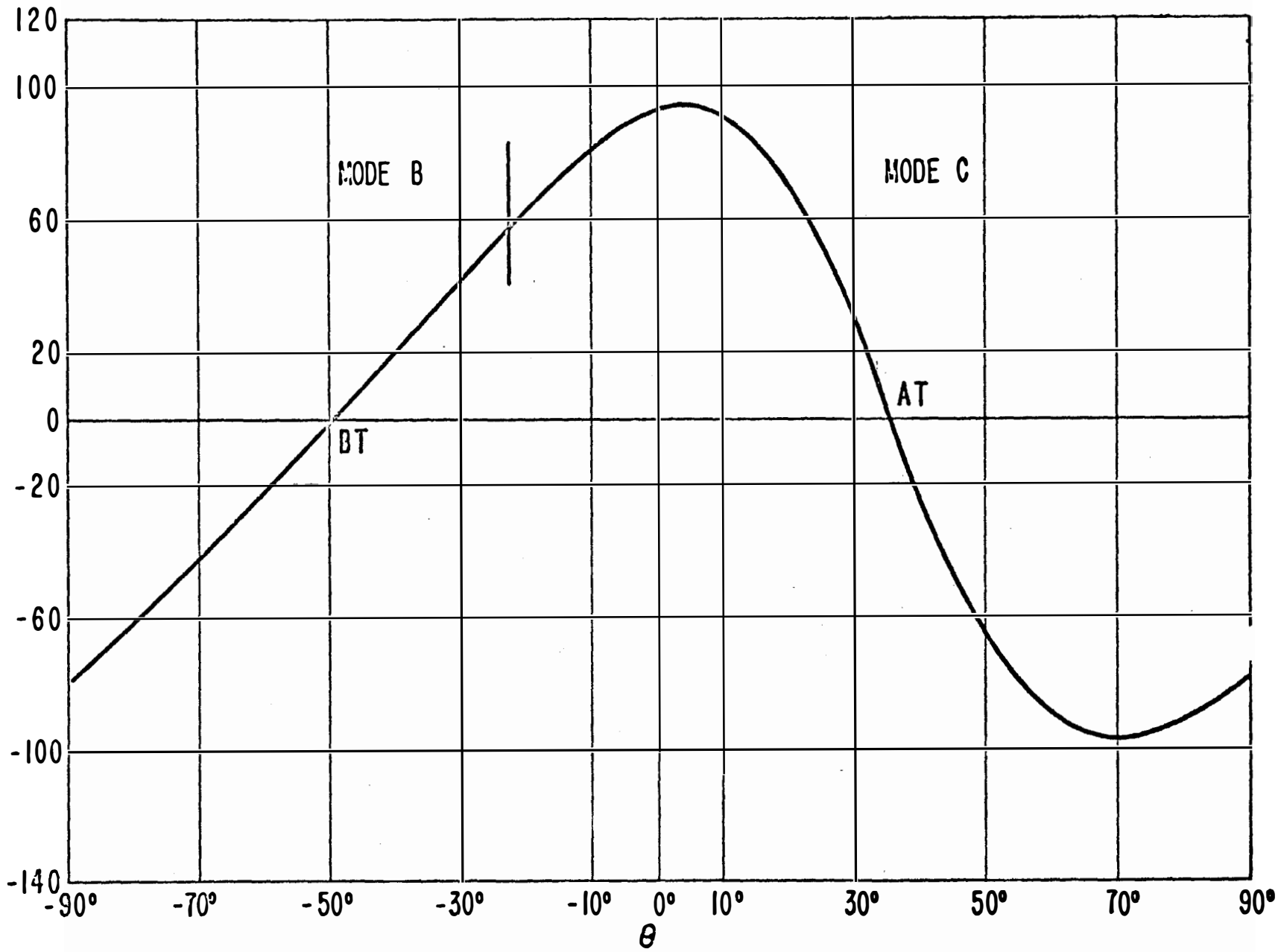

Fig. 26. First-order temperature coefficient of frequency for the plate (yx ℓ) θ vibrating in thickness modes as a function of the angle θ.

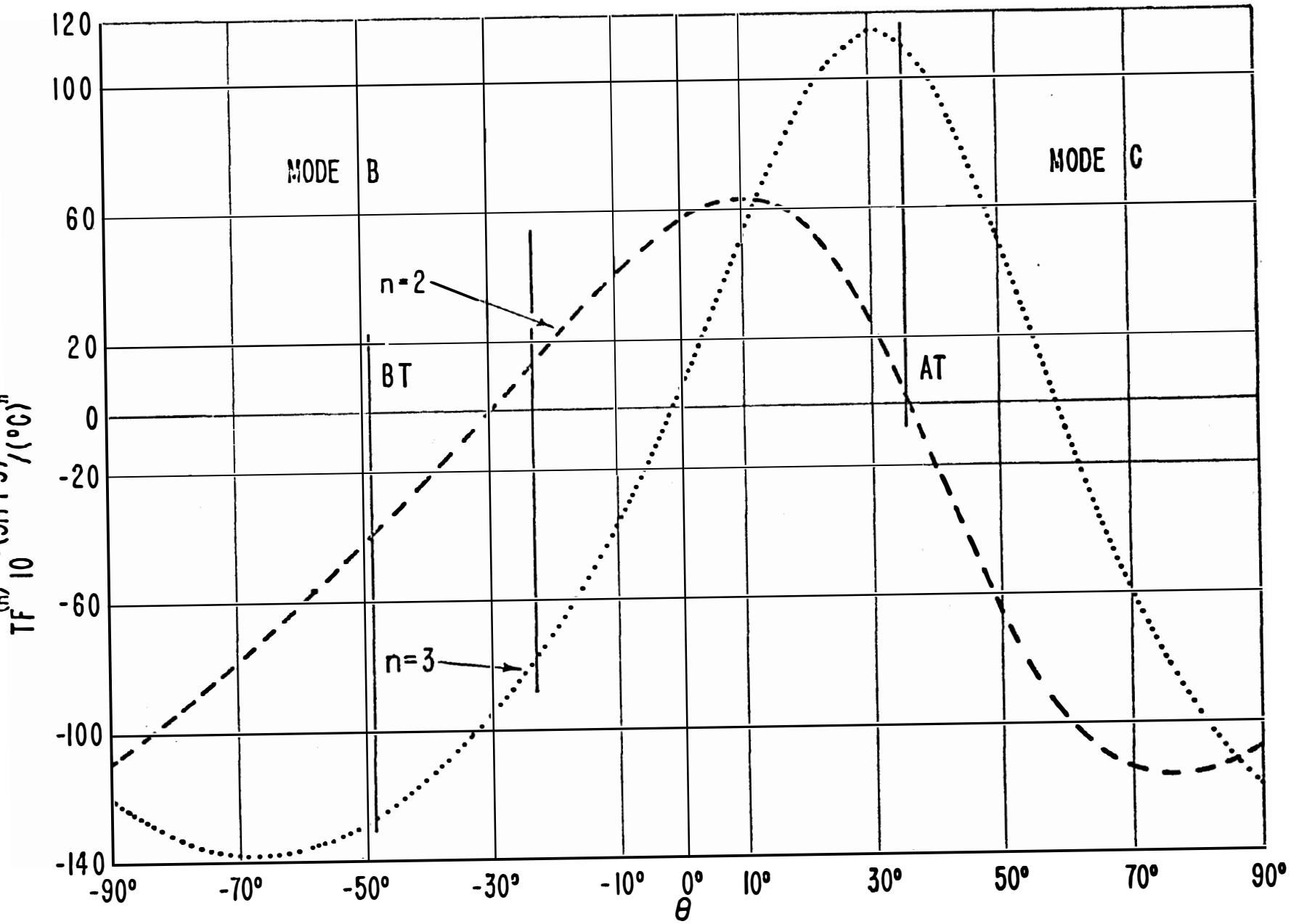

Fig. 27. Second- and third-order temperature coefficients of frequency for the plate (yxℓ) θ vibrating in thickness modes as a function of the angle θ.

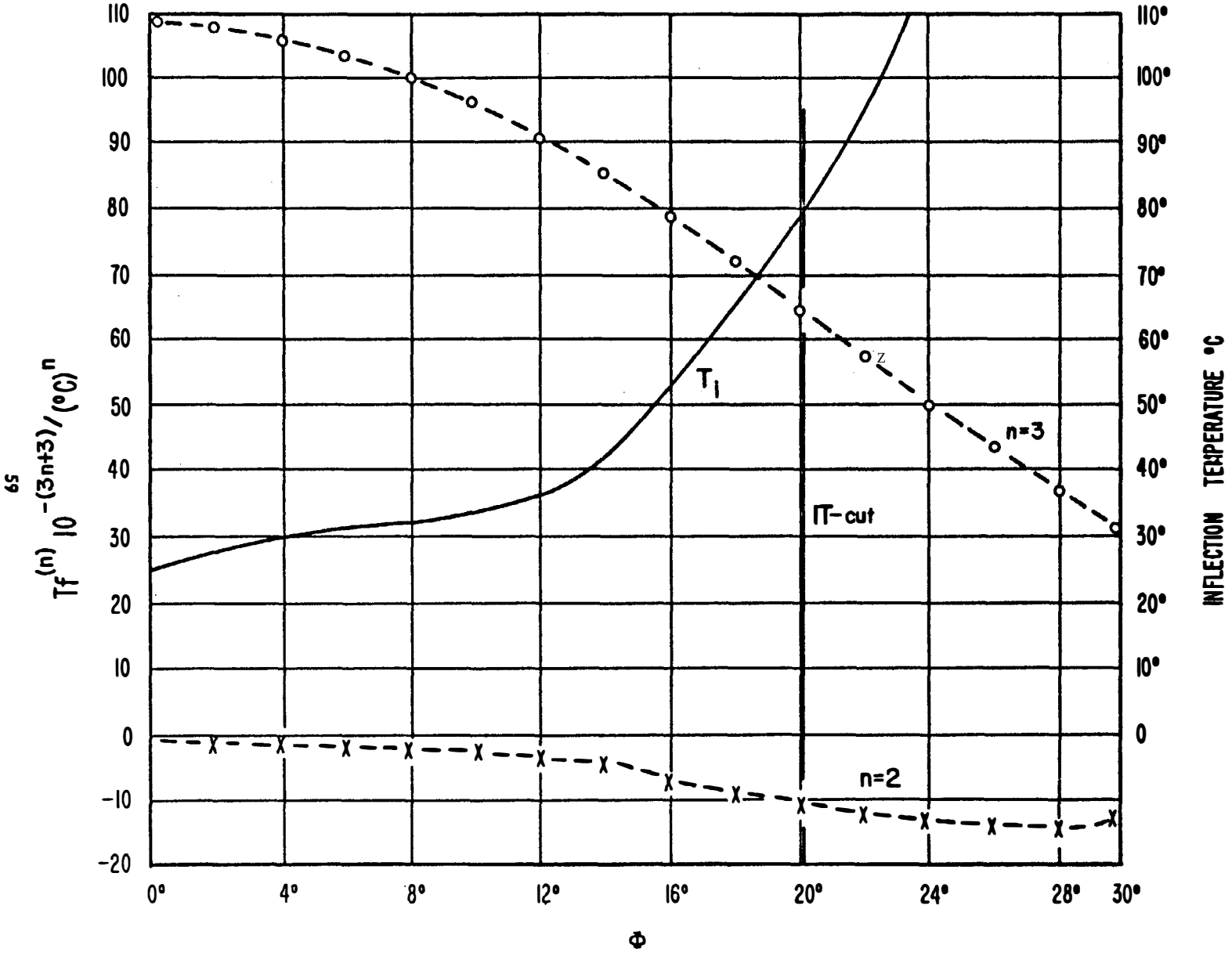

Fig. 28. Second- and third-order temperature coefficients of frequency when $Tf^{(1)} = 0$ as a function of ϕ at positive angles of θ and the inflection temperature T_i.

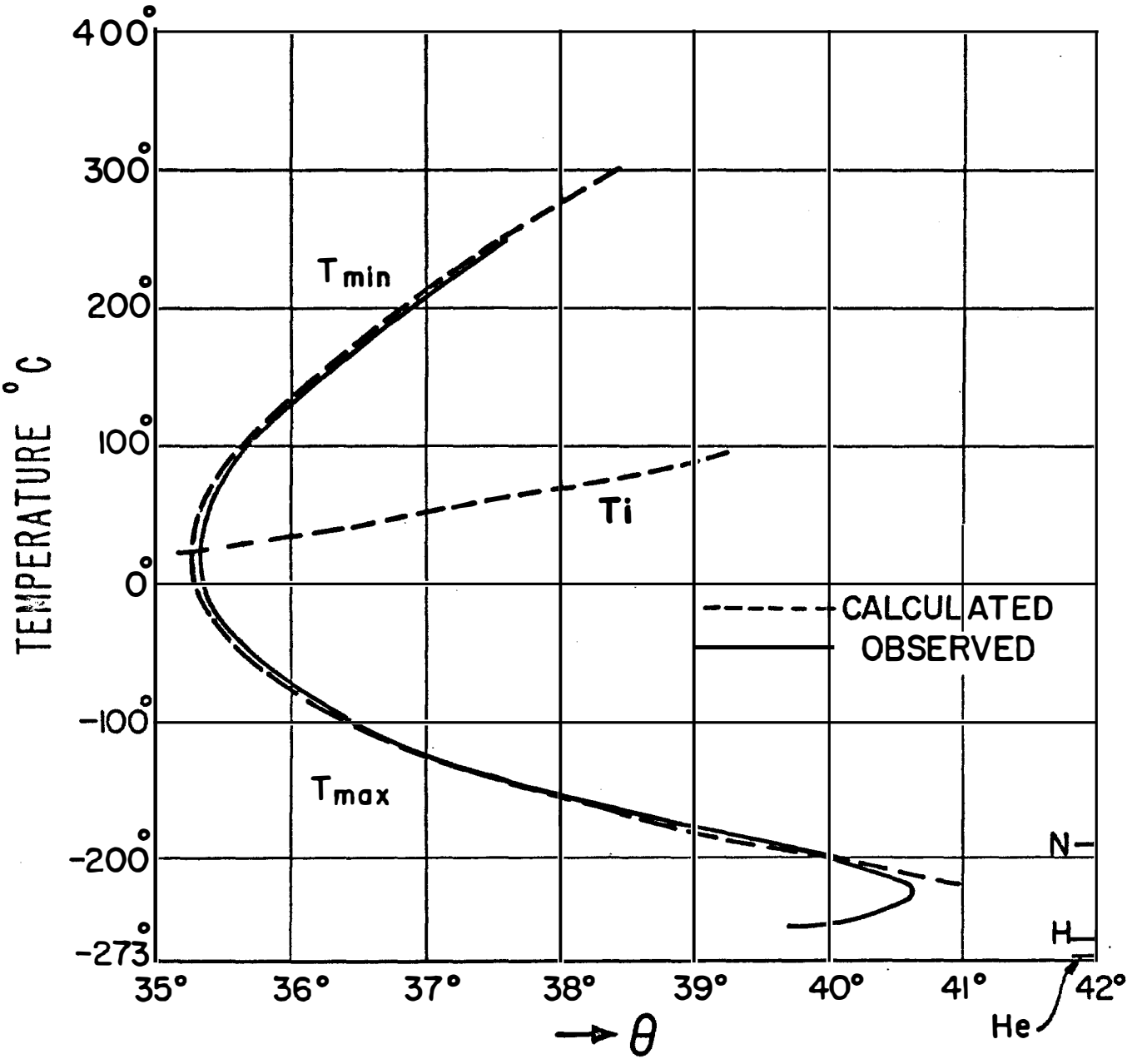

Fig. 29. Observed and calculated temperature of zero temperature coefficient of frequency vs the orientation angle θ for the AT cut.

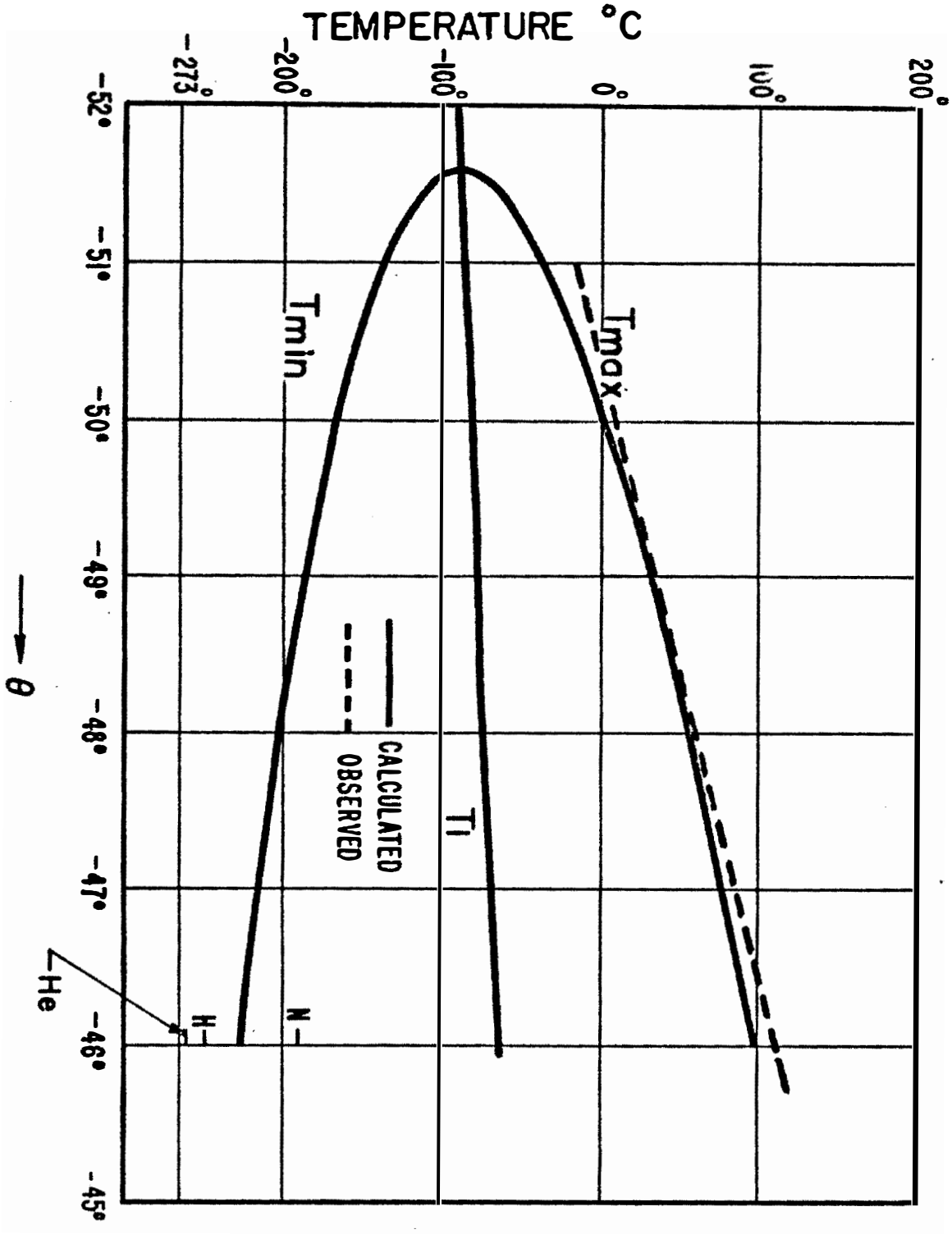

Fig. 30. Observed and calculated temperature of zero temperature coefficient of frequency vs the orientation angle θ for the BT cut.

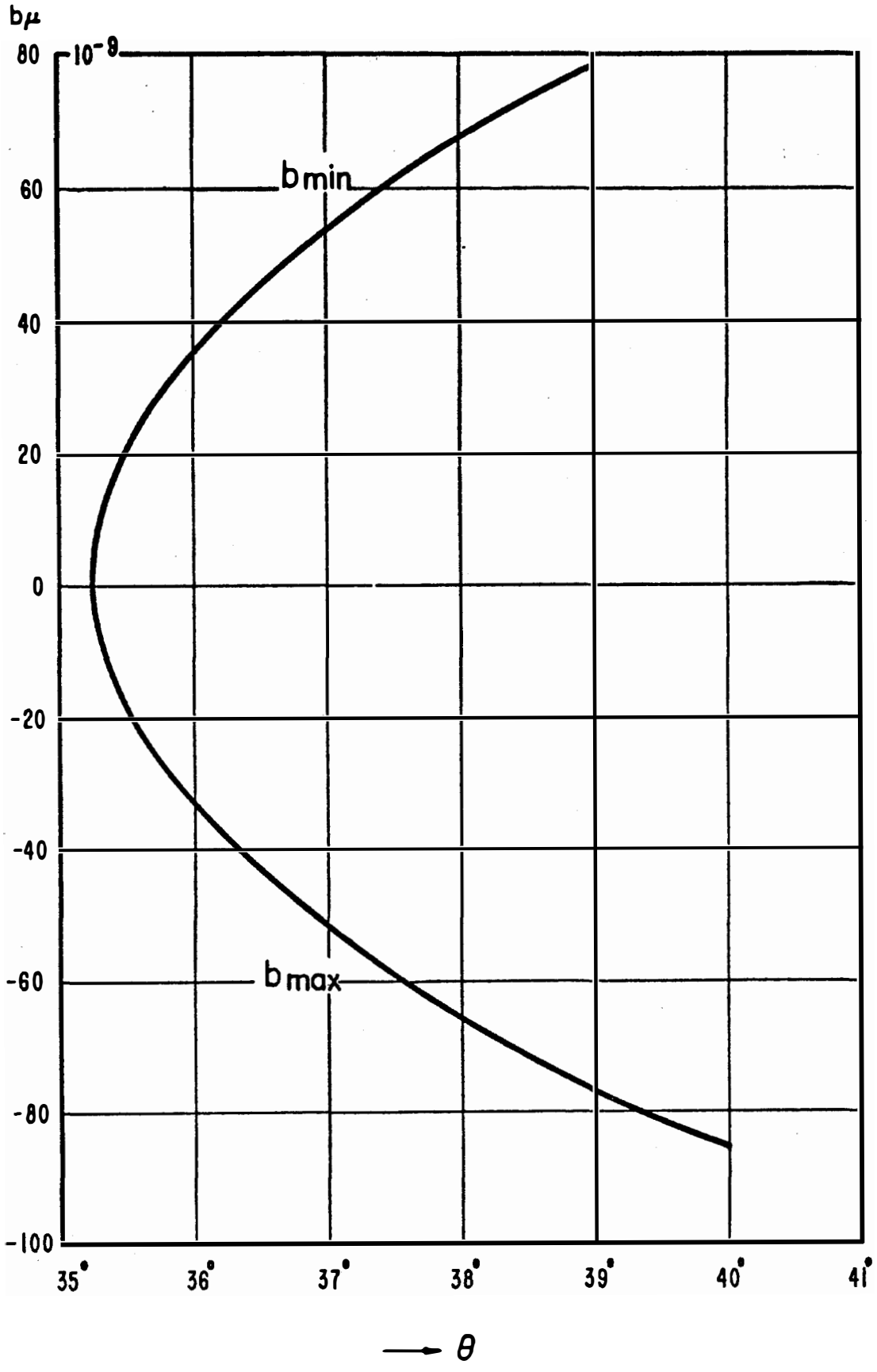

Fig. 31. Calculated values of the parabc b_μ n $10^{-9}/(°C)^2$ for the AT cut as a function of the orientation corresponding to the zero temperature coefficient curve of Fig. 26.

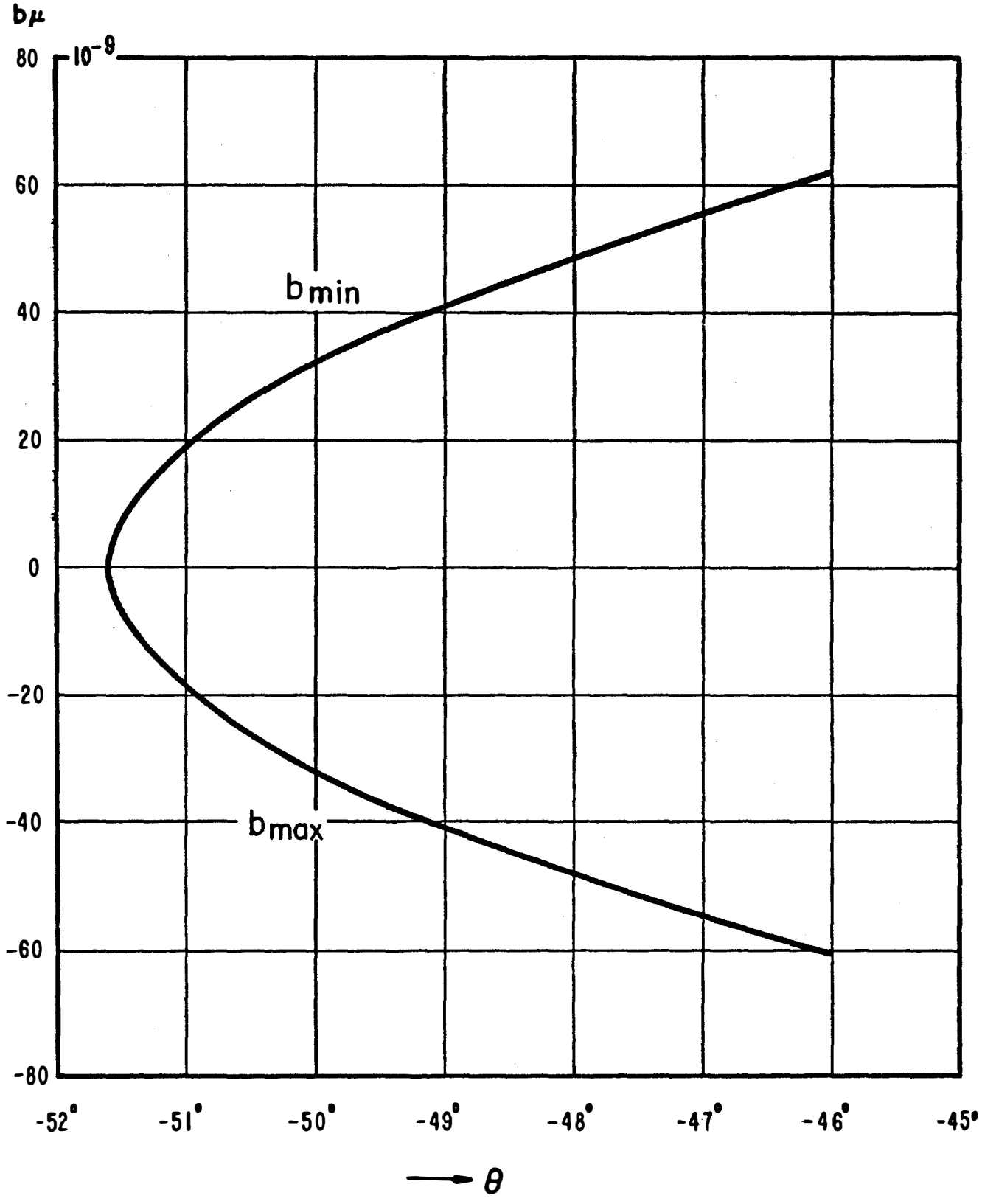

Fig. 32. Calculated values of the parabola constant b_μ in $10^{-9}/(°C)^2$ for the BT cut as a function of the orientation θ corresponding to the zero temperature coefficient curve of Fig. 26.

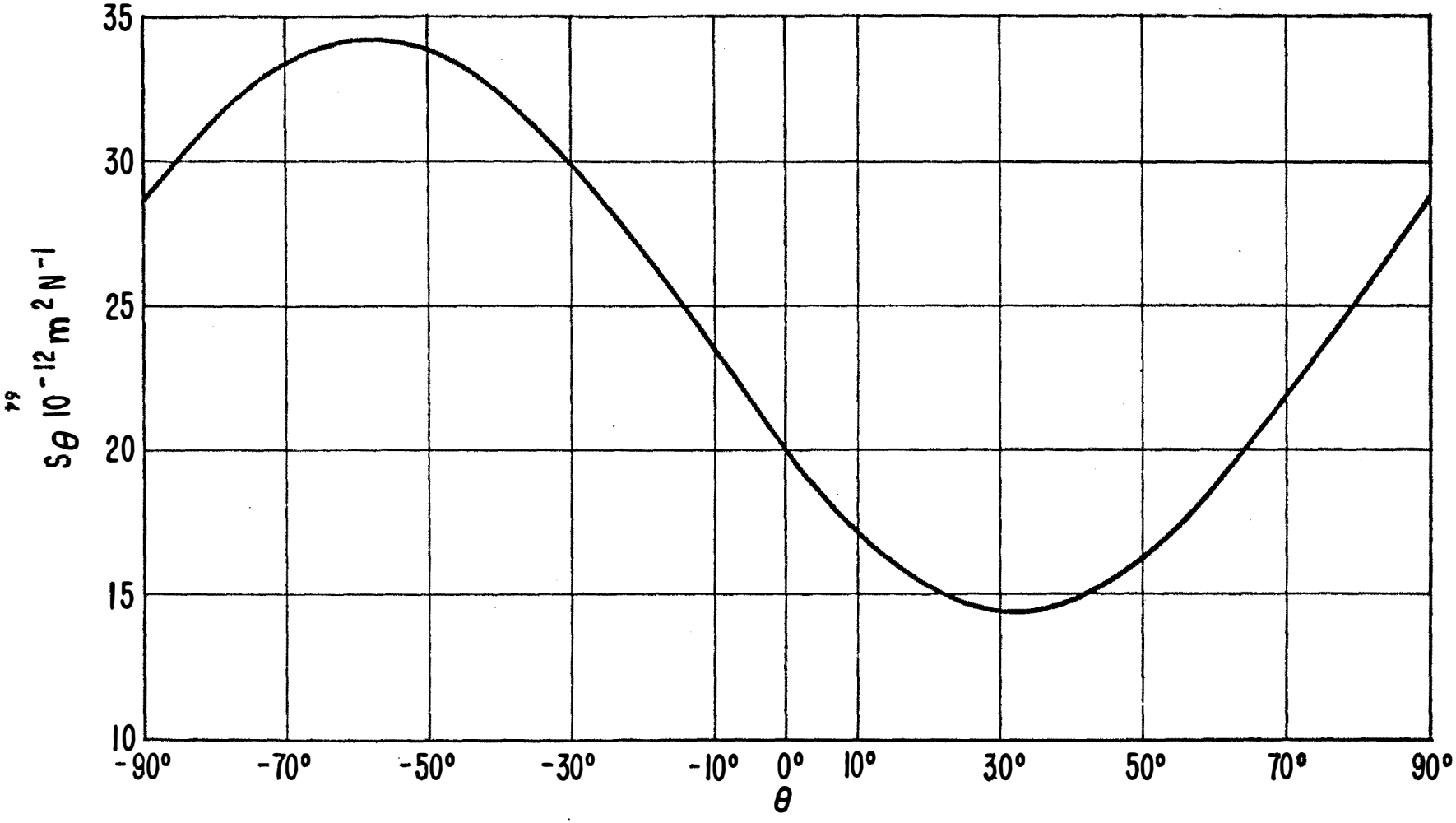

Fig. 33. Elastic compliance s'_{55} ($= s'_{44}$) for rotation (yxℓ) θ as a function of the angle θ.

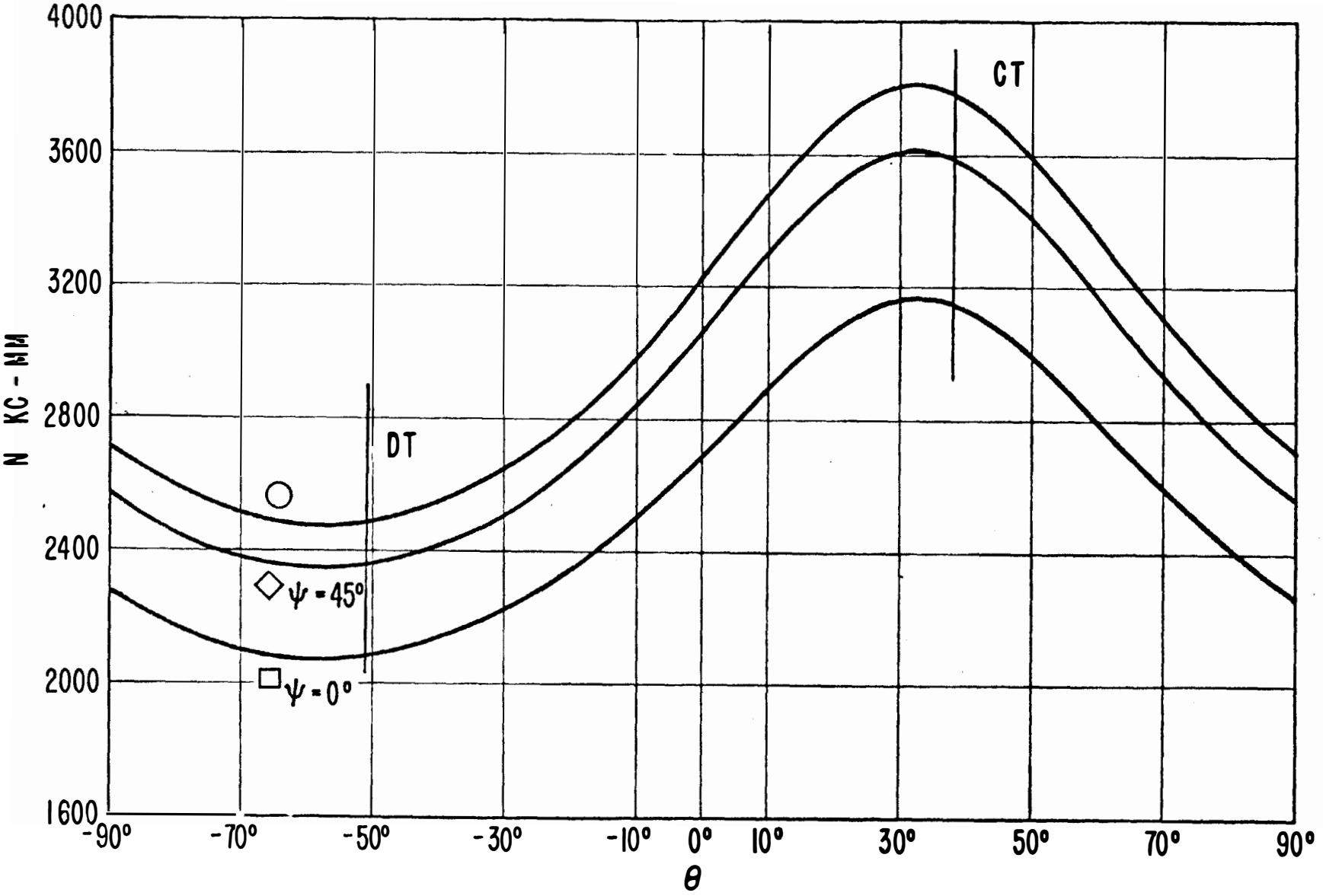

Fig. 34. Frequency constants N for the contour modes $Y_{\theta 0°}$, $Y_{\theta 45°}$, $Y_{\theta O}$ for plates (yxℓ) θ as a function of the angle θ.

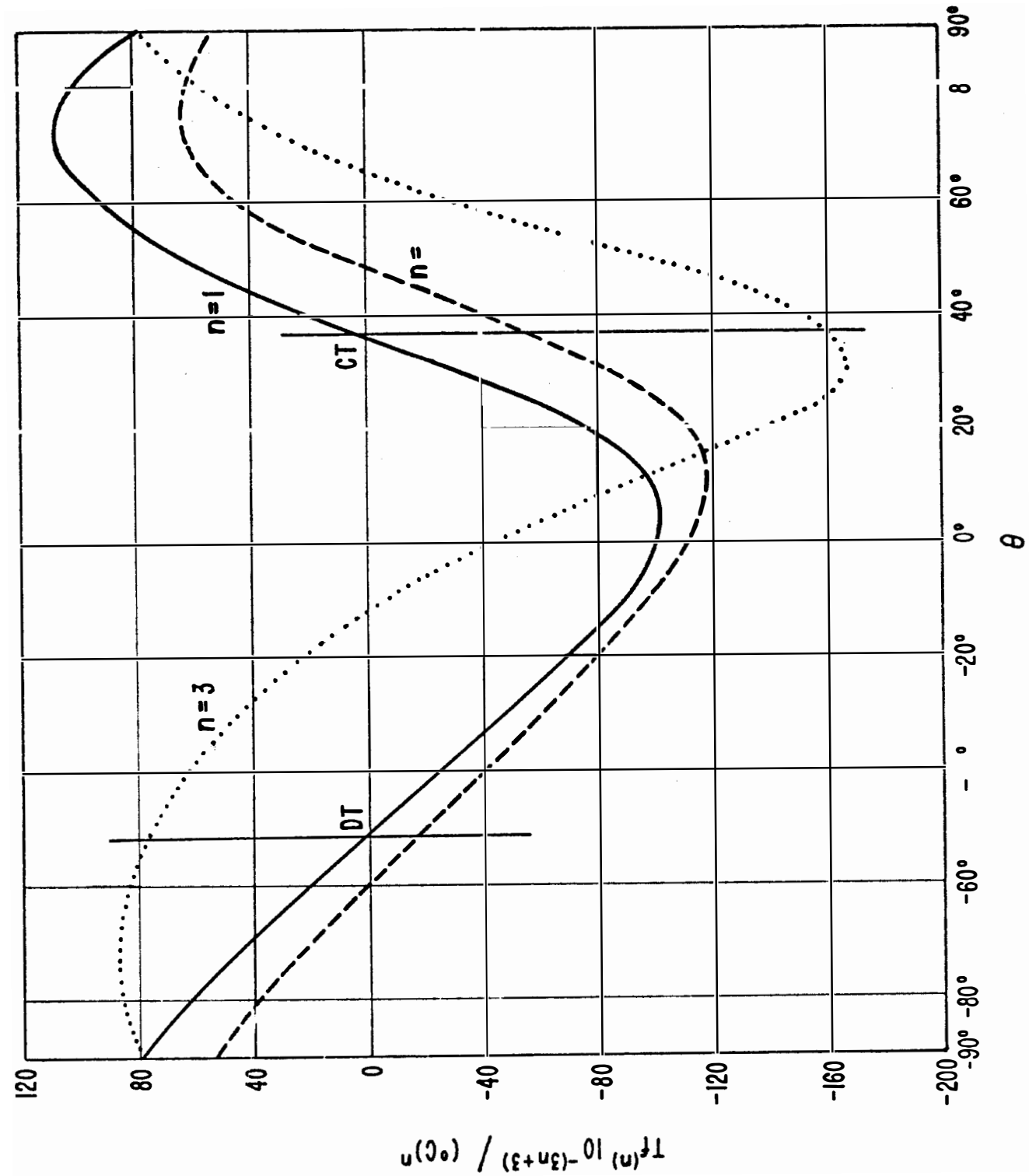

Fig. 35 First-, second- and third-order temperature coefficients of frequency for the plates (yx ℓ) θ vibrating in contour modes as a function of the angle θ

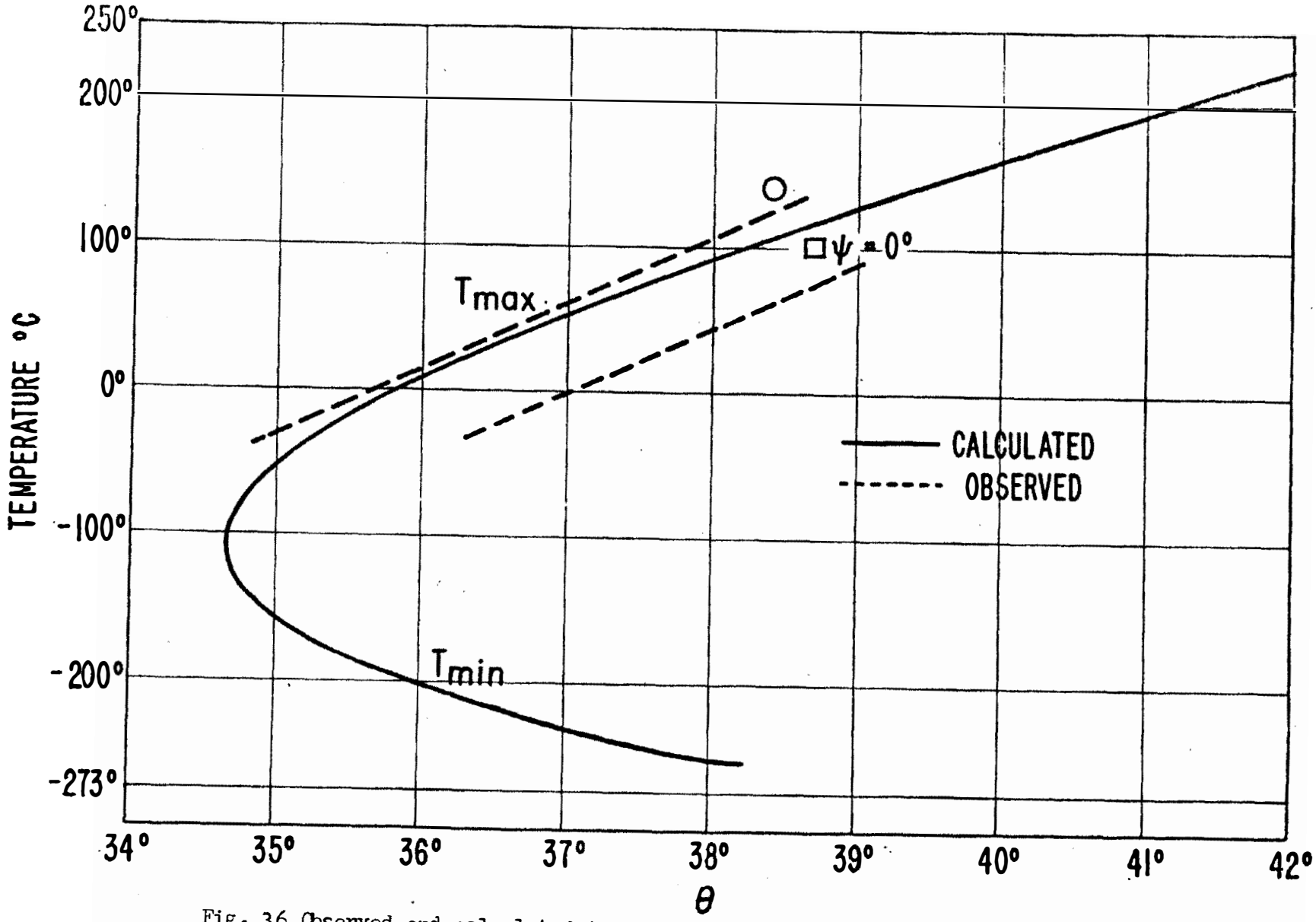

Fig. 36 Observed and calculated temperature of the zero temperature coefficient of frequency first order vs. the orientation angle θ for the CT-cut

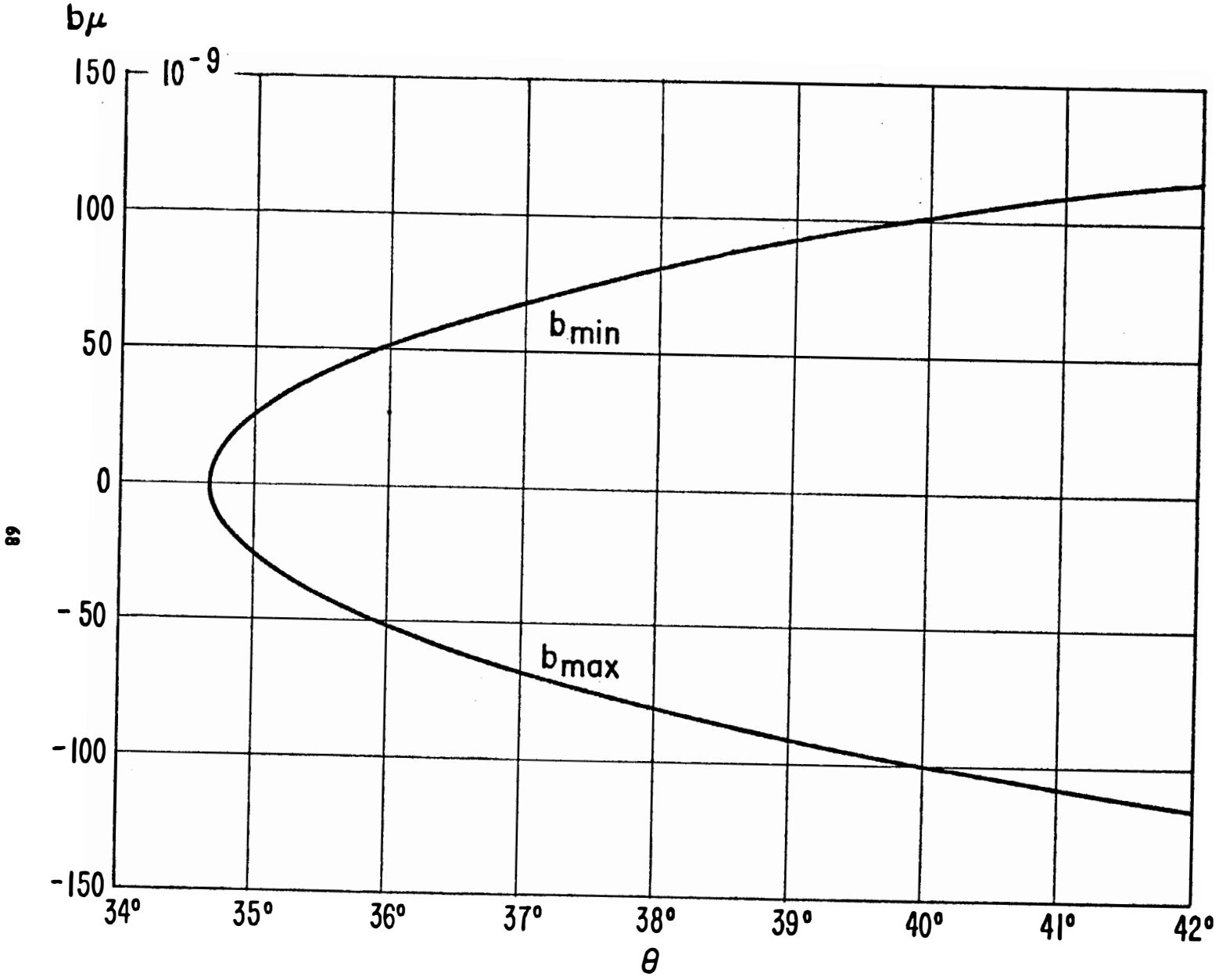

Fig. 37. Calculated values for the parabola constant b_μ in $10^{-9}/(°C)^2$ for the CT cut as a function of the orientation θ corresponding to the zero coefficient curve of Fig. 35.

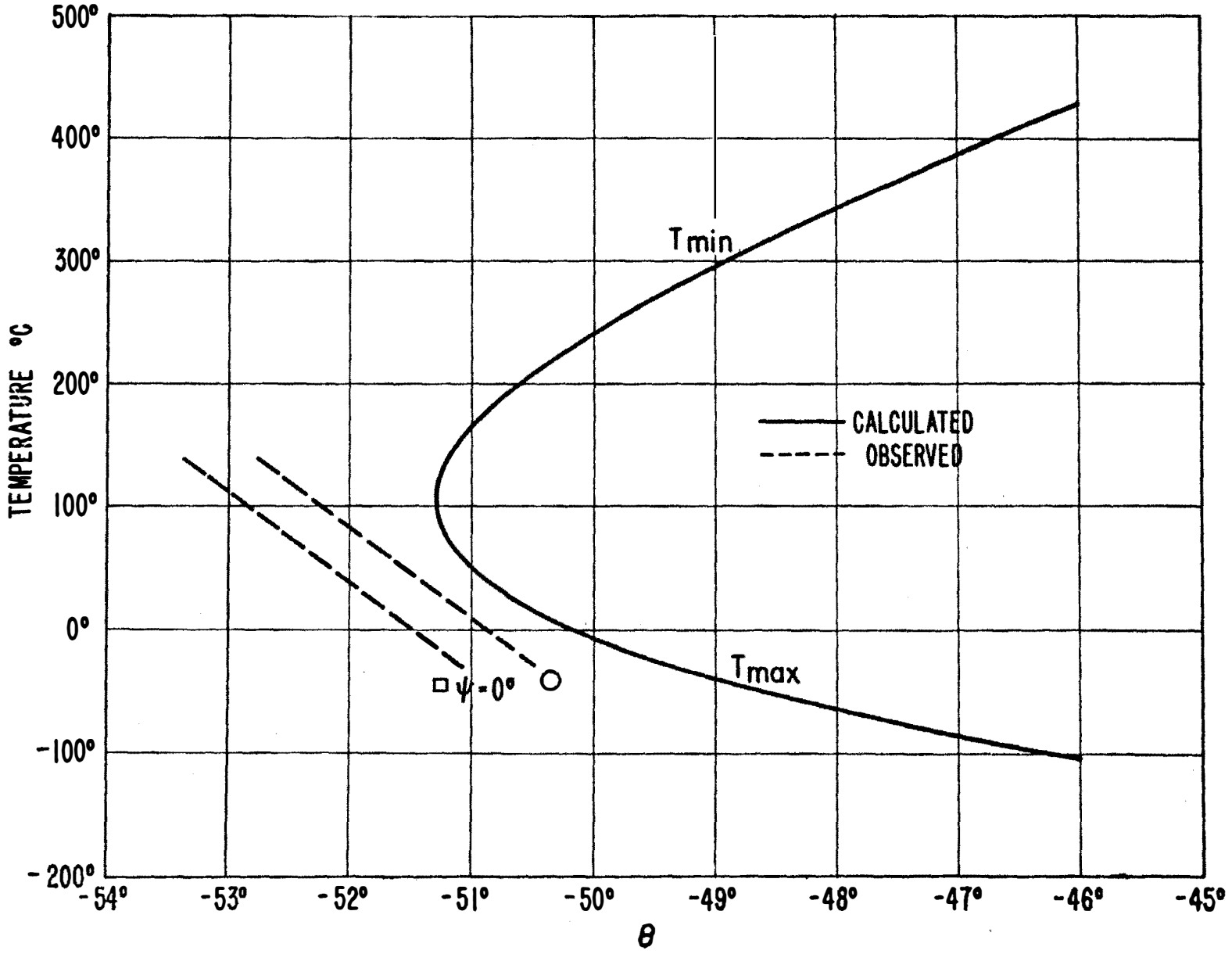

Fig. 38. Calculated temperature of zero temperature coefficient of frequency vs the orientation angle θ for the DT cut.

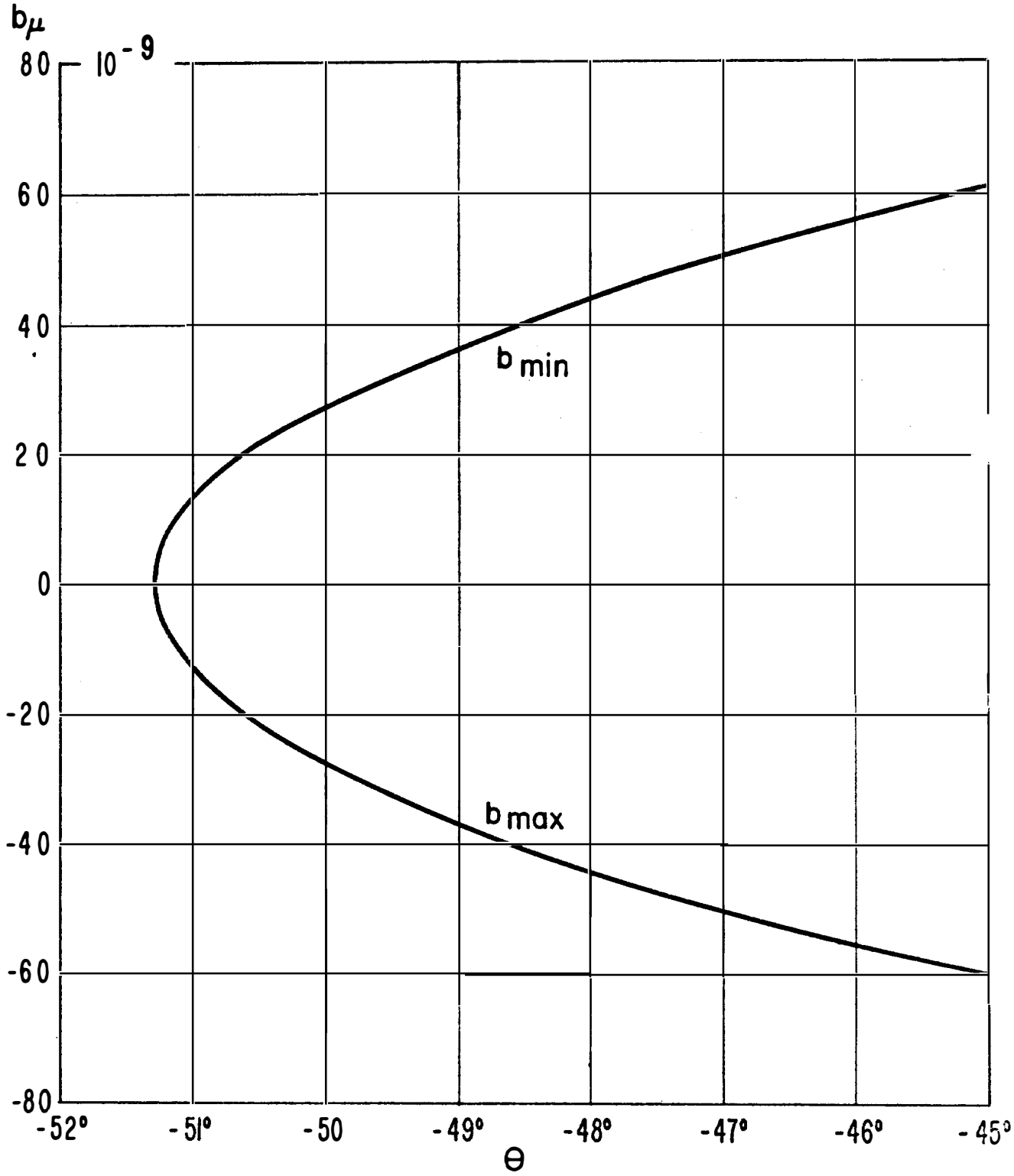

Fig. 39. Calculated values for the parabola constant b_μ in $10^{-9}/(°C)^2$ for the DT cut as a function of the orientation θ corresponding to the zero coefficient temperature curve of Fig. 35.

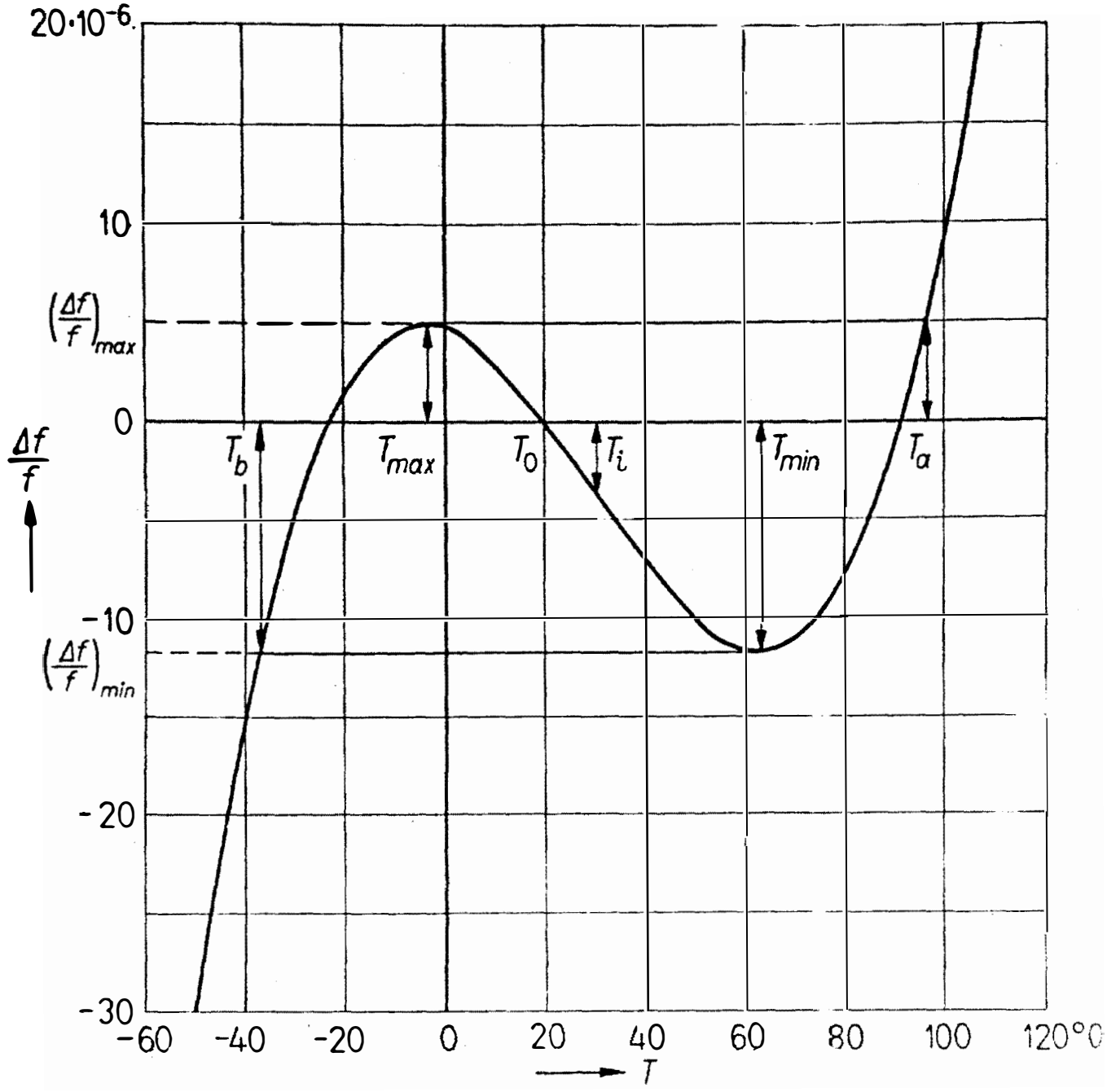

Fig. 40 Schematic frequency temperature behavior of an AT-cut in the vicinity of the first-order temperature coefficient θ